

STRUCTURAL AND GEOCHEMICAL CONSTRAINTS ON THE EMPLACEMENT OF THE MONAKOFF OXIDE Cu-Au (-Co-U-REE-Ag-Zn-Pb) DEPOSIT, MT ISA INLIER, AUSTRALIA.

¹Garry J. Davidson, ²Brett K. Davis and ¹Andrew Garner

¹*Centre for Ore Deposit Research (CODES SRC), University of Tasmania, Hobart, Tasmania, Australia.*

²*Geology Department, James Cook University, Townsville, Queensland, Australia.*

Abstract - Within the Eastern Succession of the Australian Mount Isa Inlier, Monakoff is a 1 million tonne (mt) Mesoproterozoic, oxide Cu-Au deposit only 13 km from the large (167 mt) Ernest Henry mine. The two deposits share similar geochemical signatures (Ba-Cu-Au-U-Pb-Zn-As-Sb-Co-W-Mo-Mn-F-REE), suggesting commonality of origin. This signature is far more complex than those of most other Eastern Succession Cu-Au oxide systems, but it is extremely similar to the signatures of some recently discovered large Brazilian examples, such as Alemão. Monakoff ore has a barite-carbonate-fluorite-magnetite-chalcopyrite-dominated mineralogy, and contains economic quantities of Cu, Au, Co, U and Ag; the 1–2% levels of both Pb and Zn are unusually high for oxide Cu-Au deposits. However, it lacks the distinctive K-feldspar alteration halo of Ernest Henry. It occurs on the northern south-dipping limb of the Pumpkin Gully Syncline, considered to be a regional, EW-oriented, D2 fold, bounded to the north and west by D1 thrust contacts. A splay of the northern thrust hosts the main Monakoff mineralisation. Naraku Batholith elements outcrop ~2 km north of Monakoff; and ore alteration records post-ore hornfels recrystallisation.

Two lenses of mineralisation occur: the main Monakoff Western Zone, which is a sub-vertical sheet within the shear, and the Monakoff Eastern Zone, which replaced meta-dolerite in the core of a tight D2 fold adjacent to a D1 shear, forming a narrow west-plunging pipe of unknown depth extent. A 10–20 m wide symmetric alteration halo grades inward from carbonate spotting and garnet overgrowths in regional muscovite-quartz-plagioclase schist, through biotite-spessartine-magnetite-plagioclase, to chlorite-spessartine-magnetite. This zoned sequence overprints an earlier biotite-magnetite alteration system that was focussed upon the D1 shear. A large F anomaly extends into adjacent amphibolites and porphyroblastic garnet-biotite schists, at least 130 m across strike, expanding the geochemical halo by more than 10x the dimensions of the observed alteration. The Monakoff Shear experienced movement during the regional D1 and D2 to D2.5 events. Dextral shear during D1 was the major fabric-forming event. Ore formation was synchronous with D2.5 on the basis of: (1) pseudomorphing of earlier fabrics by the ore and alteration assemblage; (2) crenulation of the biotite alteration by D3; (3) preferential development of some ore phases (carbonate, sulphide) in D2.5 crenulations; (4) a lack of pressure-shadowing on alteration garnets; and (5) use of D2 fold structures as fluid conduits. Although evidence mainly favours an epigenetic timing for mineralisation, the footwall shows evidence of minor pre-deformational Mn-Al-K-Fe metasomatism, associated with BIF formation.

Our Monakoff ore formation model involves flexural slip and production of dilatancy in broad, near-horizontal, D2.5 folds, a mechanism which accounts for the sheet-like ore geometry in vertical beds. Flexural slip was concentrated on the lubricated D1 shear system, with packages of ore fluid being drawn in by extensional failure at various scales. The geometry of extension during D2.5 favoured the inflow and mixing of fluids from above and below. As at Ernest Henry, mixing deposited barite, U-phases, carbonate, Mn-minerals, and fluorite; the components of these phases are not effectively transported and deposited from one fluid. The metals and oxidised S were carried in a corrosive, F-rich, >500° C magmatic vapour and fluid, which condensed in, and reacted with, reduced K-Ca-Ba-Mn-Cl-rich waters, as well as Fe²⁺-rich assemblages in the wallrocks, such as pre-existing magnetite.

Editor's note: This paper has been included to report the details of an important integrated, structural and geochemical study by two major research centres. It provides new insights into the formation of iron oxide copper-gold mineralisation within the Mount Isa Inlier, and by inference with other major deposits and districts around the world with similar geochemical signatures. Monakoff's significance is not in its size or economic value, but in what it can contribute to the understanding of this style of mineralisation. It has been mined and studied since well before the discovery of the nearby much larger Ernest Henry orebody, which has both similar and contrasting but complementary characteristics.

Introduction

Monakoff, which outcropped in the Proterozoic Soldiers Cap Group 20 km ENE of Cloncurry (in NW Queensland, Australia) has long been regarded as a significant ore deposit in the Mt Isa Eastern Succession, with an indicated reserve of 1 mt (million tonnes or 'metric tons') @ 1.5% Cu and 0.5 g/t Au (Milner, 1993). It is distinguished by its association with iron formation, its unusual Ba-Cu-Au-U-Pb-Zn-As-Sb-Co-W-Mo-Mn-F-REE geochemistry, and its barite-carbonate-dominated mineralogy. The metal association is extremely similar to that of the large Ernest Henry deposit (167 mt @ 1.1% Cu and 0.54 g/t Au; Mark et al., 2000), which lies only 13 km to the north. In the Mount Isa Inlier, other geochemically similar but sub-economic occurrences are known at Milo, Dairy Bore and Blockbuster-Mobs Lease (Davidson, 1998). Globally the metal association closely resembles that of the recently discovered Alemão copper-gold deposit (Carajás, Brazil), as well as having many geochemical features in common with Olympic Dam (Australia), Igarapé Bahia (Brazil) and Salobo (Carajás, Brazil) (Ronze et al., 2000; Reeve et al., 1990; Tazava and Oliveira, 2000; Souza and Vieira, 2000). Most other Cu-Au occurrences in the Mt Isa Inlier, such as Starra, Mt Elliott, Eloise, Osborne and Mt Freda, (Fig. 1;

Rotherham, 1997; Garrett, 1992; Baker, 1998; Adshead, 1995; Davidson, 1998), lack Ba-Mn-As-Sb-F-U-REE-Pb-Zn enrichment. This paper aims to provide a detailed geological, mineralogical and geochemical context for the Monakoff deposit, and to gain a greater insight into the mechanism of formation of these geochemical groupings amongst oxide Cu-Au deposits. Our findings are based upon logging of 3 deep diamond drill holes (Ashley, 1983), detailed field mapping of a 1.5 x 0.5 km area, magnetic susceptibility measurements, major and trace element profiles, examination of spatially oriented thin sections, and a compilation of previous mineral exploration and research (Ashley, 1983; Laing, 1991; Milner, 1993).

Stratigraphy and Regional Geology

The Eastern Succession consists of poly-deformed Palaeo- and Mesoproterozoic volcano-sedimentary sequences that were intruded by voluminous granite batholiths at 1540–1500 Ma (Williams and Narku Batholiths; Pollard et al., 1998, Wyborn, 1998). All sequences were deposited in intracontinental rift settings, though the relationship between some sequences is obscured by the deformation history, and is the subject of continuing detailed research. Thin skinned deformation (~1600 Ma to 1520 Ma) of the Isan Orogeny resulted in gross eastward tectonic transport (Macready et al., 1998), interleaving of major lithostratigraphic units, and a dominant north-south tectonic grain. Deformation is conventionally divided into: (D1) large-scale thrusts and isoclinal folds; (D2) major north-south upright to inclined isoclinal fold trains; and (D3) brittle-ductile spaced NW and NE-trending corridors of faulting, kinking, and folding. Major epigenetic hydrothermal activity was largely coincident with granite intrusion, and with brittle-ductile deformation phases of the orogeny. It produced regional sodic-calcic metasomatism and globally significant oxide Cu-Au deposits (De Jong and Williams, 1995; Mark, 1998; Williams, 1998). Large sediment hosted Zn (Dugald River) and Broken Hill-Type Pb-Zn-Ag deposits (Cannington, Pngmont) also occur within the Eastern Succession.

Two sequences predominate in the Monakoff area: the Soldiers Cap Group (1660–1680 Ma; Page and Sun, 1998) of the informally defined Maronan Supergroup (Beardsmore et al., 1988), and the Corella Formation of the Mary Kathleen Group (~1740 Ma; Page, 1988). Surface geology and seismic interpretation indicates the two to always be in tectonic contact (Beardsmore et al., 1988, O'Dea et al., 1997). The two major contacts are the Cloncurry Overthrust and the Pumpkin Gully Fault. In fact the Cloncurry Overthrust changes from a single NW-trending strand south of Cloncurry, to several NE-trending *en echelon* segments and splays (including the Pumpkin Gully Fault) north of Cloncurry. Regionally, the outcropping Soldiers Cap Group north of the Weatherley Creek Syncline differs from equivalent stratigraphy further south in its low metamorphic grade (greenschist transitional to amphibolite; Ashley, 1983, Rubenach and Barker, 1996), and less intense structural fabrics; consequently many primary igneous and sedimentary structures are preserved.

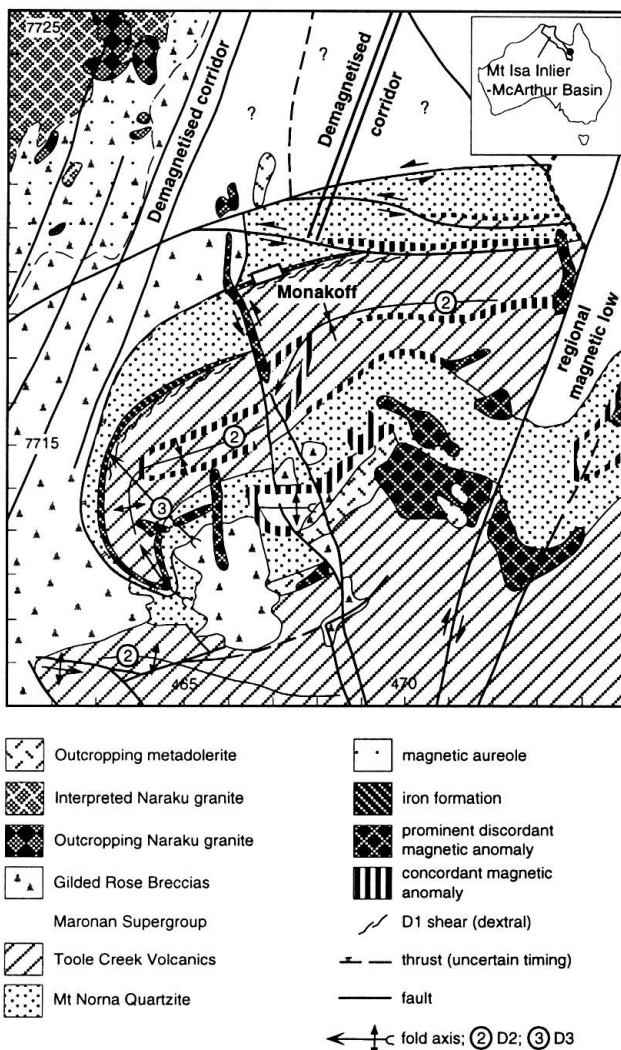


Figure 1: Interpreted geology modified after Ryburn et al. (1988), constructed using aeromagnetic data.

The Soldiers Cap Group is a conformable carbonate-poor stratigraphic succession younging from the Llewellyn Creek Formation (pelite, arenite), through the Mount Norna Quartzite (quartzo-feldspathic arenite, carbonaceous pelite, metagreywacke, metabasalt, iron formation) to the Toole Creek Volcanics (metabasalt, minor carbonaceous metasediment, iron formation) (Derrick et al., 1976). Dolerite sills and dykes were widely intruded, largely prior to the main metamorphism, in some cases prior to consolidation. These were followed by the Corella Formation which consists of well bedded scapolitic carbonate and quartzo-feldspathic layers, inferred to have been deposited within a shallow marine to evaporitic shelf environment (Reinhardt, 1986); it is widely suggested to have been a major source of saline fluids during metamorphism (eg., Oliver, 1995). Where it is strongly intra-formationally brecciated it is referred to as Corella breccias (Ryburn et al., 1988), and where it is brecciated and contains exotic clasts it is referred to as Gilded Rose breccia, considered to be hydrothermal in origin (Marshall and Oliver, 2001).

Cu-Au mineralisation is hosted mainly within the Soldiers Cap Group, with only minor occurrences adjacent to or within the Corella Formation breccias within 1 km of more significant accumulations. The dominant Cu-Au mineralisation styles in the Cloncurry area are:

- 1). replacement Cu-Au-U barite-siderite lenses associated with iron formations, of which Monakoff is the largest known example;
- 2). brittle Mt Freda-style carbonate vein and replacement deposits;
- 3). albitite-associated vein and replacement deposits;

4). brittle-ductile quartz vein and vein networks, subdivided into a). Gilded Rose-type, and b). Eloise-type (Davidson, 1998).

Monakoff occurs within an unusual east-west trending, south-younging belt of Soldiers Cap, which is separated from Corella breccia to the north and west by D1 thrust contacts. The deposit occurs on the northern south-dipping limb of the D2 Pumpkin Gully Syncline, on a tectonic contact between the Mount Norna Quartzite and the Toole Creek Volcanics (Ashley, 1983). This position corresponds to a regionally extensive linear magnetic anomaly, with sporadic iron formations and ironstones as its outcrop expression. Approximately 1 km west of Monakoff, the ore stratigraphy is off-set by ~500 m across a sinistral, sub-vertical, north-striking fault which can be traced magnetically southwards through the Pumpkin Gully Syncline down to a major fault intersection close to the Matilda Highway (Fig. 1). This fault is of interest because it hosts intrusive calc-silicate breccia bodies, and contains carbonate-quartz breccia veins similar to those that host Mount Freda-style mineralisation (Davidson, 1998). Around 3 km of the fault has a positive magnetic expression near Monakoff. A second set of east-west faults and fault-splays, again with sinistral offset, are visible in aeromagnetic images some 1 to 2 km north of Monakoff. These are interpreted to repeat the ore horizon several times to the north-east under cover. A fault with an orientation and offset that is consistent with this fault generation separates the Monakoff West Zone from the Monakoff East Zone of mineralisation (Fig. 2). No granitic intrusives have been identified at Monakoff. The nearest granites, 2 km north of Monakoff, are outcropping sentinels of the Naraku Batholith, with the main metamorphic aureole to the batholith occurring a further 2 km NW (Fig. 1).

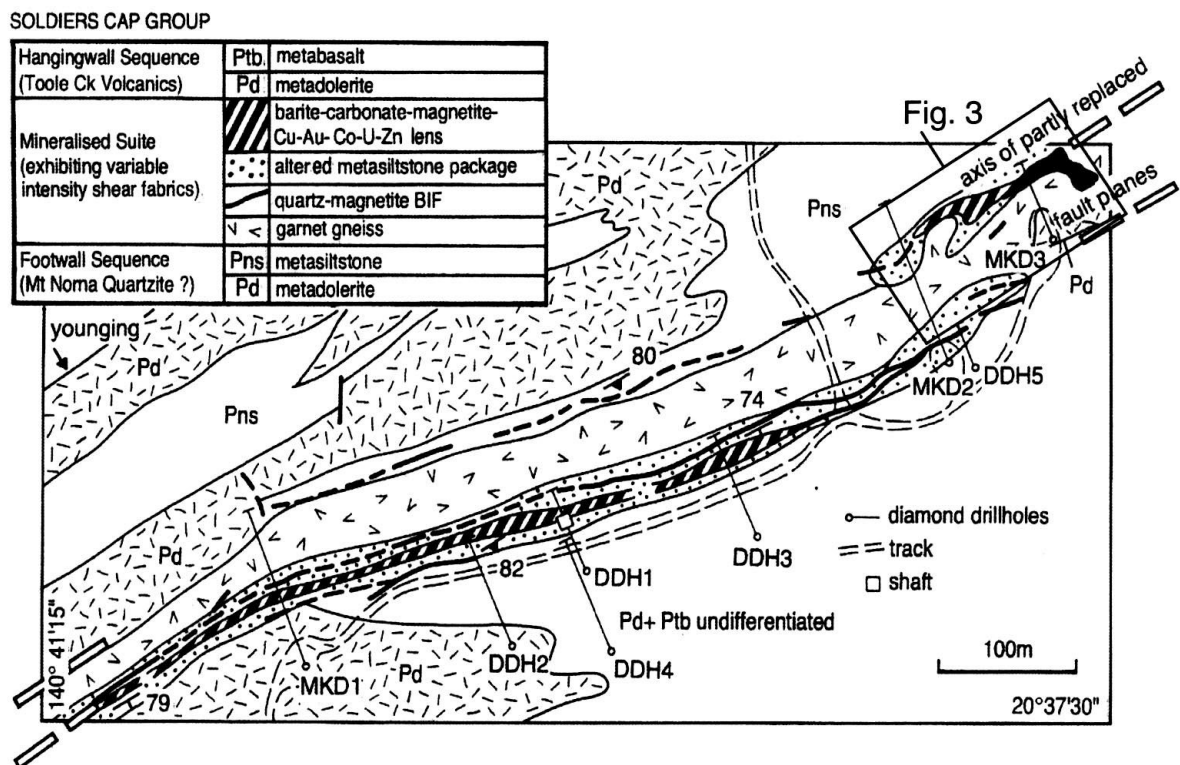


Figure 2: Monakoff prospect geology, modified after Ashley (1983)

Deposit Geology

Discovered by prospectors prior to 1908, Monakoff was drilled in several phases by companies between 1954 and 1997, including Gold Mines of Australia (3 holes, one shaft), Mount Isa Mines (2 holes), Esso Minerals (3 holes) and Cloncurry Mining (30 shorter holes during mining delineation). Most exploration programs adopted a syngenetic ore genesis model because of the sheet-like

nature of the ore. Laing (1991) briefly interpreted Monakoff as an epigenetic ironstone-hosted deposit at the conjunction of a D1 mylonite and a later structure. Cloncurry Mining removed approximately 300 000 tonnes by open pit mining, ceasing operations in 1997. The deposit stratigraphy was originally preserved in a low 1 km long ridge, now partly removed by mining, rising 30-40 m above the plains to the north. Outcrop is moderate in the footwall, good to excellent in the ore stratigraphy, and moderate in the hangingwall.

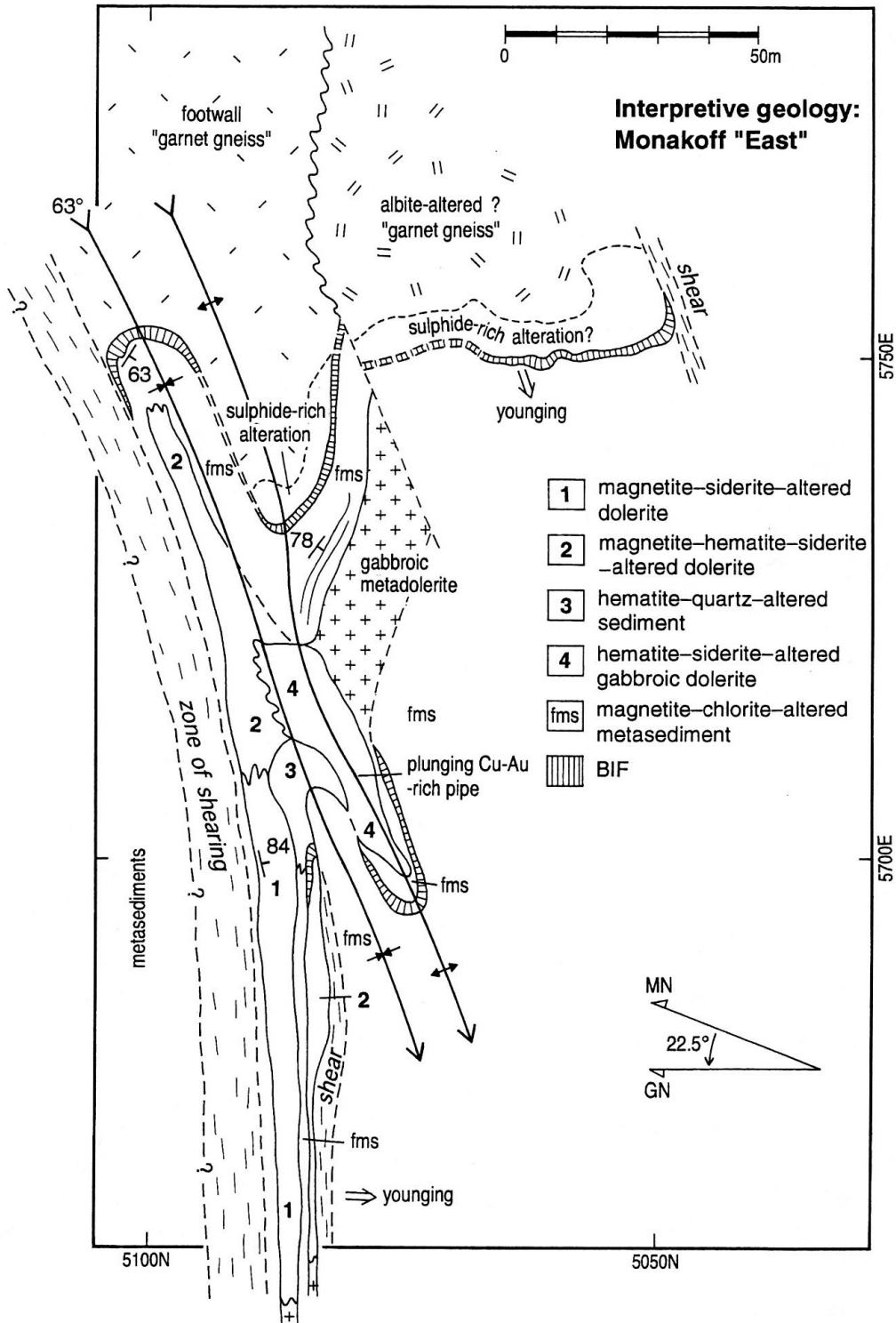


Figure 3: Interpretive map of the Monakoff East Zone mineralisation, emphasising the fold hinge control on the replacement of a meta-dolerite. The factual surface map is presented in Davidson (1995).

Footwall

The upper 100 m of footwall lithologies comprise intercalated magnetite-bearing muscovite pelites, psammopelites, and meta-dolerites of the uppermost Mount Norna Quartzite, overlain by massive porphyroblastic garnet-biotite schist, then a persistent iron formation, and lastly by strongly sheared metasediments immediately hosting the Monakoff West ore. The metadolerites form continuous sills with locally angular contacts and variable epidote alteration, particularly adjacent to sediment contacts. Most also either preserve peperitic margins or contain peperitised silicified sediment for 0.2–1.0 m away from their margins (Plate 1b), indicating that they intruded un-lithified host sediment (Davidson and Davis, 1997; Hatton et al., 2000). The pelites, which dominate the upper 100 m of Mount Norna Quartzite stratigraphy at this location, contain only fine 1–3 mm laminations, which may be either sedimentological or tectonic in origin. Conversely, psammo-pelites are present below 100 m as 0.5 m thick graded beds containing cross-bedding, plane lamination, convoluted bedding, flame structures and rip-up clasts, all consistent with a turbiditic emplacement origin and indicating upward-facing stratigraphy. The predominant metamorphic assemblage in the sediments is muscovite-plagioclase-quartz-magnetite±tourmaline.

The porphyroblastic garnet-biotite schist (Plate 2a) is mainly massive, with randomly oriented lathes of plagioclase, and a lower peperitic contact indicating an intrusive origin during lithification. However, the upper 3–5 m contains quartz-magnetite-filled vesicles consistent with an extrusive coherent lava origin. Thus a partly intrusive, partly extrusive igneous origin is indicated. Ashley (1983) favoured an andesitic parentage for this unit, with significant pre-metamorphic Si-K-Fe-Mn alteration to account for the mineralogy. Detailed geochemistry (see “geochemistry” section) confirms that the unit is far more felsic than the majority of igneous products in the Toole Creek Volcanics, possessing high field strength element abundances that are consistent with an andesitic to dacitic precursor.

The continuous, thin (1–2 m), prominently banded, quartz-magnetite±hematite BIF can be traced through the whole prospect ~5–10 m above the top of the porphyroblastic garnet-biotite schist, hosted by pelitic metasediment. Bands vary from 1–2 mm wrinkly lamination (possibly crenulations; Plate 2b), to 0.5 cm interbands of quartz-barite, and spessartine-magnetite. The unit regularly and preferentially contains F1, F2 and F3 micro- to meso-scale folds (Plate 2e), which is evidence that it formed prior to any regional deformation. Approximately 3 km west along strike from Monakoff, iron formations at this stratigraphic position are interbedded with sedimentary or hydrothermal carbonate beds 30 cm thick, all folded by D1-folds (Plate 2e). Ryburn et al. (1988) describe stromatolitic structures in carbonates of this horizon. This association has not however been recognised at Monakoff. BIF defines the major D2 fold structure hosting the Monakoff East Zone, where it is also enclosed in places by carbonate-barite

alteration (Fig. 7). The Monakoff West Zone mineralisation consistently occurs 20–30 m above the BIF (Fig. 2, and detailed geological maps in Davidson and Davis 1996), although the BIF is strongly anomalous in most ore elements. The immediate footwall and hangingwall to ore are bedded and strongly sheared fine to medium-grained, dark-grey magnetite-bearing siltstones.

Several minor transgressive lithologies occur in the footwall. These include: 1). areas of variable muscovite-alteration, particularly associated with orthogonal fractures, which become more abundant westwards; 2). north-south oriented ‘pebble’ dykes, with clasts of sericitised wallrock, and matrices of albite-actinolite-carbonate-sulphide (weathered), together with parallel calcite-siderite-muscovite-scapolite-quartz-chalcopyrite veins up to 0.5 m thick (Plates 1f & 2c); and 3). one isolated, 30 m diameter outcrop of “Gilded Rose” breccia approximately 200 m north of the main shaft at Monakoff, which field relations indicate to be vertical and intrusive. The carbonate-bearing veins are magnetite destructive and have halos in core that extend away from the vein for ~10x the vein-width (Plate 1f). This vein generation also occurs on lithological contacts west of Monakoff, where its orientations indicate an emplacement during strike-slip movement. Their lack of deformation indicates a D3- to post-D3 timing.

Hangingwall

A 20–30 m thick interval of short strike-length metabasalts, minor iron formation, volcanic conglomerate, breccia-bearing limestone, and meta-dolerites occur immediately above the thin strip of sheared metasediment that hosts ore. A local spectacular pillow breccia outcrops close to the ore package near the centre of the deposit, although this was not encountered in core. Ryburn et al. (1988) also report black carbonaceous limestone and stromatolitic chert from this stratigraphic position, but these lithologies were not observed by the authors. More common elements of the Toole Creek Volcanics occur above this complex facies assemblage, consisting of massive medium to coarse-grained meta-dolerite to gabbro in the west, and mixed meta-dolerite, meta-basalt, siliceous siltstone and minor iron formations in the east. Unlike the upper Mount Norna Quartzite, no regional spessartine-biotite alteration is present in the hangingwall. Epidote alteration is present inhomogeneously along thin vein zones and particularly along mafic unit contacts, where it may form 1–5 m wide epidote-quartz pods. Along-strike from the Monakoff mineralisation, a zone of this material is deformed by D1 structures, suggesting that it is a pre-deformational alteration type. In core, small post-metamorphic biotite-carbonate-magnetite veins occur that appear to be mineralogically similar to some parts of the ore package alteration.

“Ore Package”

Ashley (1983) considered the “ore package” to include the altered rocks adjacent to the ore, the ores themselves, and the overlying sediments and basaltic tuff, all younging and

dipping southward (Fig. 2). It consequently includes some units already described above. Ryburn et al. (1988) defines the base of the Toole Creek Volcanics at Monakoff as the top of the ore “package”, or the base of the first meta-basalt/meta-dolerite above the ore. The ore package contains two structurally separate mineralisation zones: 1). Monakoff East, which has a steep pipe-like geometry, and was not included in the quoted ore reserve; and 2). Monakoff West, which was mined and has the form of a steeply dipping sheet. Monakoff East is slightly deeper in the stratigraphy than the Monakoff West Zone.

Near-ore alteration commences in the footwall with distinctive porphyroblastic spessartine-biotite-quartz-plagioclase-chloritoid-tourmaline-biotite development in the meta-andesite (Plate 2a), in which the idioblastic garnet is disseminated or forms irregular bands localised on peperite zones. In places pink spessartine is overgrown by coarse-grained almandine + quartz, indicating that Monakoff peak metamorphism exceeded the almandine isograd. It is not certain if almandine stability was attained during regional D2, or whether it occurred during a local contact metamorphic effect that developed during intrusion of an unexposed granite. However, almandine does provide an important time constraint on spessartine growth, which itself required a Mn-rich stratigraphy or fluid for growth. Chloritoid has a randomly oriented distribution, and contains a magnetite-defined foliation, S1 or S2.

Post-peak metamorphic alteration is abundant above the garnet-biotite schist, exhibiting zoning around the ores, low-angle shears, and tension gashes. The general alteration sequence spanning scales of from 0.5 to 10 m distant from mineralised zones is an outer chlorite-spessartine (Plate 3e), inward to biotite-magnetite \pm pyrite, to siderite-magnetite \pm pyrite alteration as ore or sulphide-bearing veins/fractures are approached. In meta-siltstones this alteration forms pseudo-breccias (Plate 1a, 3g), in which ‘clasts’ have distinct dark biotite-rich centres. Carbonate alteration also preferentially affects thin basaltic dykes or extrusives. The general complexity of the fabrics are heightened by probable peperitic relationships, pillow basalt fabrics, and autoclastic brecciation that formed during volcanism.

A constraint on timing of ore and alteration is provided by a 1.5 m wide post-ore dyke in MKD2 (Fig. 2), which is not

exposed in outcrop. This dyke contains only minor chlorite alteration of olivine, but is chilled against barite-chalcocopyrite ore on one hand, and severely altered dyke host rock on the other. Furthermore, barite-carbonate ore is metamorphosed at the dyke contact, producing 1 cm long siderite porphyroblasts. Insufficient K was present in the dyke to obtain an Ar-Ar age estimate. However, a lack of ore-related alteration indicates that the dyke post-dates D2.5 (see structural section) and could be part of the Lakeview Dolerite swarm (~1100 Ma) which intrudes parts of the Mount Isa Inlier. It plots in the sub-alkaline basalt field ($Nb/Y \sim 0.30-0.34$) of Winchester and Floyd (1977), ie. more alkaline than the small surrounding amphibolite host rock population ($Nb/Y \sim 0.1-0.2$), assuming that the relative abundances of the high field strength element have not been altered.

Structural History of Monakoff

A multistage deformation history is well developed at Monakoff, particularly in the main ore-related shear zone and rocks bounding it. The deformation history comprises four events, herein termed D1, D2, D2.5 and D3. These correlate well with events of the same generation recognised for the Isan Orogeny regionally, although some orientations are unusual. D1 was responsible for formation of the main central shear zone, hereafter referred to as the Monakoff Shear Zone, which is apparent as a zone of S1 foliation intensification several metres to tens of metres wide that trends sub-parallel to lithological layering (bedding) within the ore package. Production of the shear zone would appear to represent deformation partitioning involving accommodation of D1 shear strain by the phyllosilicate-rich horizons between the hangingwall mafic Toole Creek Volcanics and the massive porphyroblastic garnet-biotite schist (Fig. 2), with strain enhanced dissolution causing a relative increase in the amount of phyllosilicate. Interestingly, D1 potentially comprises two phases of deformation, producing a deformation history similar to that noted by Davis et al. (2001a) in the Quamby area to the north.

S1 in the Monakoff Shear Zone is a subvertical mylonitic fabric that anastomoses around elongate, ellipsoidal pods of relatively more quartz-rich material that have

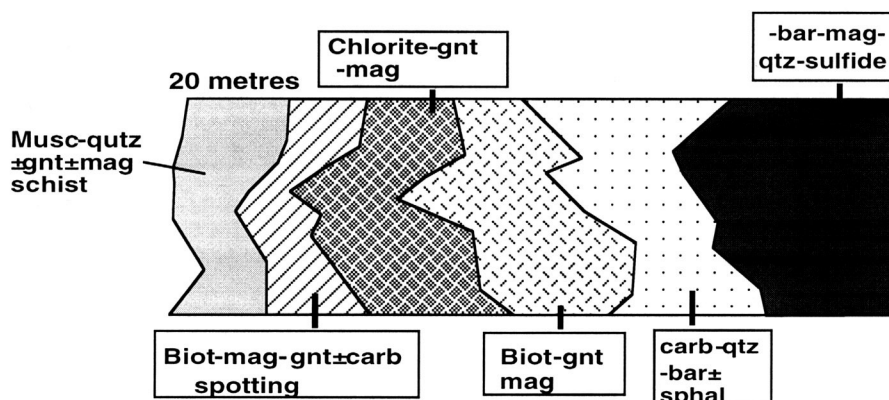


Figure 4: A schematic view of alteration types spreading away from ore on the right hand side of the figure, Monakoff Western Zone.

accommodated D1 shortening strain (Plate 1c). These pods vary in scale from centimetres to tens of centimetres, and generally have aspect ratios in plan of 2:1 to 4:1. Their extent in the third dimension is unknown. In the shear zone, the mylonitic fabric is folded about steeply plunging folds that are tight to isoclinal, and centimetres to tens of centimetres in wavelength. Microscale crenulations exhibit locally consistent asymmetries that change across cm-scale F1 fold hinges, indicating that folds and crenulations are of the same generation. These F1 folds are in turn deformed by a subvertical fabric that is continuous with, but distinguishable from, that interpreted to represent the regional S2 fabric. As such, there appears to have been two stages of deformation comprising D1, namely formation of the main shear fabric representing the initial stage, and ongoing reactivation of this fabric during formation of the folds and micro-crenulations of the latter stage. Alternatively, fabric formation and overprinting folds represent complex patterns of repartitioning of shearing and shortening strain during progressive D1 deformation.

Maximum inter-limb angles of the folds produced during the second stage of D1 are of the order of 30°. These folds are generally isolated, intrafolial and rootless, although some fold couplets and triplets have been noted. Fold asymmetries are common and the dominant population indicates that sense of shear during D1 was dextral. This is in good agreement with the shear sense movement resolved from other kinematic indicators such as foliation geometries and clast asymmetries. However, west of Monakoff in the Pumpkin Gully Syncline, the axes of decimetre- to metre-scale F1 are near-horizontal, probably as a combined result of strong rotational strain in the main shear during D1 and the effect of overprinting deformation.

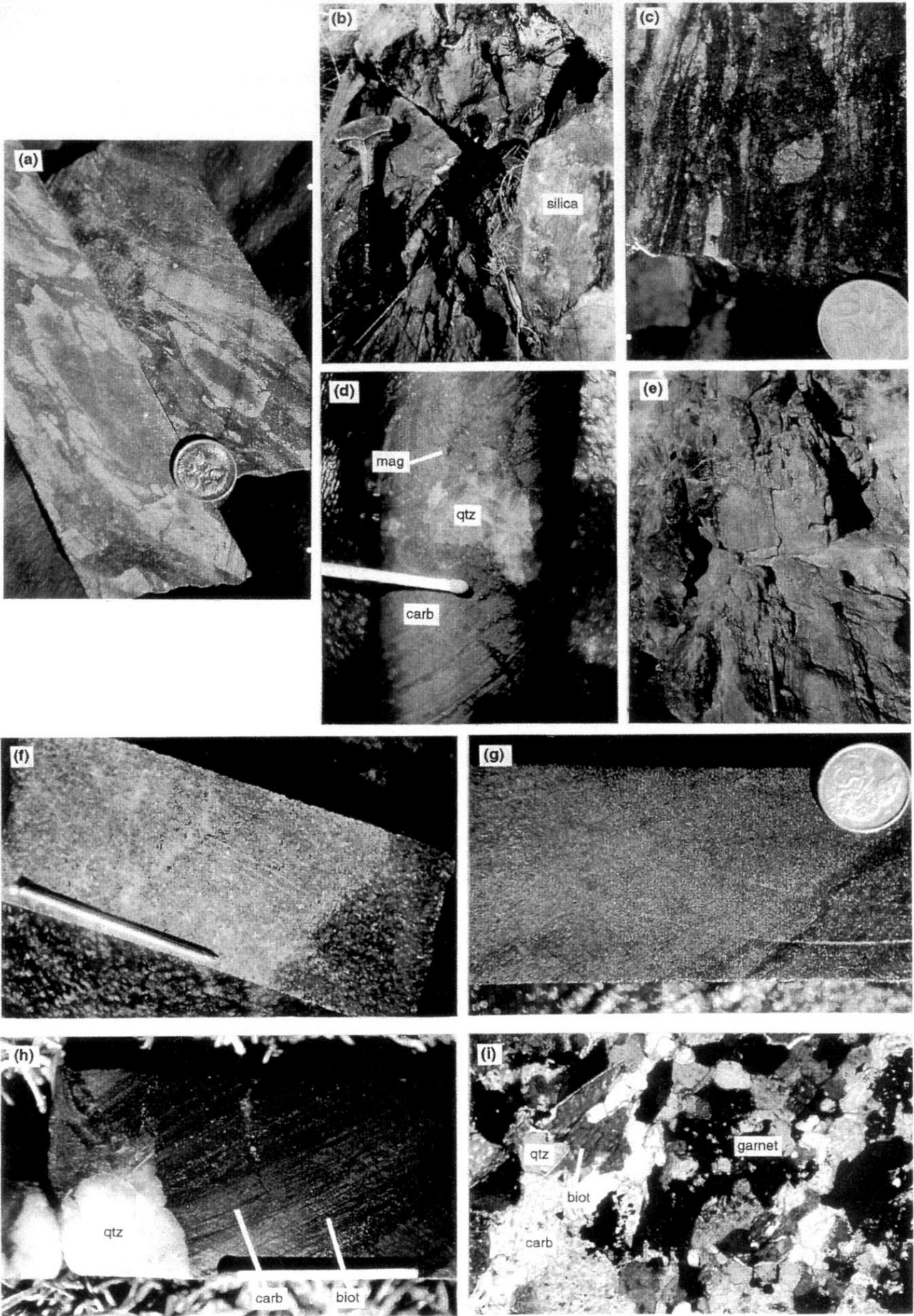
D1 kinematic indicators are best represented by foliation geometries around and within clasts (Fig. 5), and indicate an overall dextral sense of movement on the shear zone (Plate 2f). Local shear reversals, which have produced geometries indicative of sinistral shear, have also been observed but are uncommon. Dramatic volume loss was experienced by shear zone rocks and we interpret this to be due to shear enhanced dissolution of minerals such as quartz. This is evident where zones of high D1 shearing strain have impinged on individual lithological layers and caused marked reductions in thickness. Such zones of high shearing strain are most evident against large quartzose clasts where strain accumulation has occurred.

At the outcrop scale, D2 produced meso-scale folds, generally of centimetres to tens of centimetres in wavelength and amplitude. Folds vary from open to tight (Fig. 5), and commonly deform D1 folds within the central shear zone. S2 is a pervasive, approximately northwest trending cleavage that varies from a fracture cleavage to a schistosity. The similar orientations of S1 and S2 have produced a composite S1-S2 fabric, particularly on F1 fold limbs. Alignment of magnetite within this composite fabric suggests D2 growth. L_1^2 lineations are steeply plunging sub-parallel to F_1^2 fold axes. The L_2^2 stretching lineation is steeply pitching in S2. The structure of the Monakoff

East Zone is dominated by a large, steeply plunging, tight F2 fold with a wavelength of ~20 m, the hinge of which is defined by a cylindrical mineralised breccia pipe (Fig. 3). A syn- to post-D2 age of brecciation is implied by the control of the F2 hinge on the location and orientation of brecciation (although this does not necessarily imply the same age for the mineralization contained within it). Kinematics for D2 are indicated by a dominance of crenulation asymmetries exhibiting north-side-up sense of shear, which are also preserved within the core of garnet porphyroblasts. These garnet cores are interpreted to have grown syn-D2. D2.5 structures (Plates 2h, 3e) are best developed at the northern end of the deposit, particularly within zones of chlorite schist in the central shear zone. F2.5 folds are rare and restricted to open flexures. Accumulation of D2.5 shearing strain against the margins of the syn-D2 garnet porphyroblasts has rotated the D2 differentiated crenulation with a top-to-the-southwest sense of shear, producing sigmoidal and spiral foliation geometries. The rotated fabric is continuous with S2 in the early garnet cores and subsequent D2.5 growth of garnet has preserved this geometry as sigmoidal and spiral inclusion trails. Elsewhere the S2.5 fabric is pervasively developed but the earlier S2 crenulation has been destroyed, restricting fabric geometries to sigmoidal D2.5 crenulations. S2.5 is best developed within chlorite-rich zones that are associated with biotite-garnet-chlorite alteration. This alteration forms a halo to the deposit and is potentially associated with the mineralising event.

Given that the garnets are an integral part of the alteration assemblage and that the majority of them show micro-structural relationships consistent with growth during D2.5 (Plate 3e), a post-D2 to syn-D2.5 age is interpreted for the emplacement of mineralisation. Furthermore, this suggests that the D2 and D2.5 events may have been very closely spaced in time. Emplacement of mineralisation during progressive deformation is indicated by the occurrence of ore phases in oblique-chocolate block boudinage veins, observed both in core and in outcrop, with extension occurring in competent units in both near horizontal and near-vertical directions. Boudinaged neck zones in the intense metasomatic halo, or in the weakly altered host rock, generally consist of quartz vein-fill with minor garnet, monazite ± galena-pyrite-sphalerite (Plates 1d, 1h). They are surrounded by radiating fracture networks of magnetite, that cross-cut pervasive siderite replacement zones, surrounded in turn by strong biotite alteration. In outcrop, a string of such failure zones sub-parallel to bedding, and associated layer-parallel alteration, resemble original Fe-Mn-rich beds, but in fact such zones result from the preferential flow of fluids parallel to S0/S1/S2. In mineralised zones, the main boudin neck mineralogy is barite-carbonate-fluorite.

Deformation during D3 was coarsely partitioned on the meso-scale, resulting in corridors of well developed decimetre-scale folds with local intense S3 developments that are separated by zones of relatively less intense cleavage development and an almost total absence of folding (eg., 5200E, see Davidson & Davis 1996 for maps).



In the zones of intense deformation, S₃ is present as a steeply dipping, approximately north-northeast striking, crenulation or differentiated crenulation cleavage (Plate 2g). The best overprinting evidence for S₃ occurs where it has cross-cut the shallow S_{2.5}. In zones of high D₃ shearing strain, the accumulation of D₃ strain against garnet porphyroblasts has destroyed pre-D₃ geometries except in very rare strain shadows adjacent to the garnets. Locally, S₃ is present as a planar fabric displaying consistent asymmetry. This consistent asymmetry is observed on both sides of some folds, indicating that the folds are products of pre-D₃ deformation. On the limb of the earlier folds, where the asymmetry was the same as that for the late sub-vertical event, an intense composite foliation has been produced. Foliation asymmetries (crenulations, S-C fabrics) for pre-D₃ fabrics have been noted on the limbs of folds where the asymmetry of the earlier fabric was opposite to that of the late one. S₃ is also defined by crenulations in biotite alteration, and this biotite is considered part of the alteration halo to the mineralisation (see "alteration" section).

In the zones of relatively less intense D₃, zones of unfolded material between F₃ fold corridors commonly contain pre-D₃ surfaces (bedding and foliations) that have been in orientations favourable for accommodating D₃ shearing strain. In general, S₂ in zones of foliation reactivation has been deformed but not destroyed, indicating that deformation associated with this process was quite minor in many places within the deposit. This supports the view that the dextral asymmetries noted throughout the shear zone are preserved D₁ geometries, and that the shear sense during D₃ was the same as that in D₁. Depending on how the deformation was partitioned and redistributed during progressive D₃, these pre-existing surfaces accommodated both synthetic and antithetic shear relative to the overall D₃ shear sense in adjacent folded layers. The reactivation of pre-D₃ surfaces also produced apparently ambiguous structural overprinting relationships. S₁ planes that were reactivated by D₃ now lie axial planar to crenulations of S₂.

Of interest are micro-structural relationships indicating that a final stage of garnet growth occurred late-syn- to post-formation of S₃. The late planar S₃ is continuous with planar inclusion trails in the garnet rims, and deflection of the fabric at the margin of porphyroblasts is minimal to absent. The late stage of garnet growth is only detectable

via inclusion style and content. The final rim-phase of garnet growth locally occurs as elongate crystals that have grown syntaxially from zones of quartz-rich folia out into, and at right angles to, the adjacent chlorite-rich foliation zones. Magnetite crystals are generally larger in the matrix than in the garnet porphyroblasts (Plate 3e), indicating ongoing magnetite growth into the late stage of deformation and porphyroblast growth (D₃?). Furthermore, these micro-textural relationships suggest that some magnetite at least is not temporally related to mineralisation as it post-dates it.

Mineralisation

The main western ore zone forms an east-dipping sheet 700 m long x 2-10 m thick, with unknown depth extent, whereas the smaller eastern mineralisation, ~100 m northeast of the end of the western zone, forms a pipe-like body that plunges very steeply west, with a 40 m strike length at surface. Between the two zones, porphyroblastic garnet-biotite schist is replaced by unmineralised albite around a sinistral D₃- to post-D₃ fault (Fig. 3); this alteration style is not seen elsewhere in the prospect, but is regionally common around post-orogenic granites (Mark, 1998). The textures, settings and associations of the two mineralised zones are very different.

The western zone is enclosed by, and replaces, magnetite-bearing meta-siltstones. At surface it is manifested as a friable, resistant, massive unit with variable black pyrolusite and malachite staining, sometimes given the field term "garnet sandstone", on the basis of its arenaceous texture and pink colour (Plate 1e). At depth it is a remarkably massive unit compared to surrounding alteration (Plate 1g, 3a, 3b, 3c), and consists of barite, ponite (Fe-rhodochrosite; see ore mineralogy section), magnetite, chalcopyrite, pyrite, spessartine, fluorite ±K-feldspar, sphalerite, galena, arsenopyrite, mackinawite, molybdenite, brannerite/davidite, pentlandite and linnaeite (Ashley, 1983). This mineralogy gives rise to the cosmopolitan element assemblage Cu-Au-Ag-U-Zn-Pb-Co-Mo-W-Sn-F-Mn-Ba-Sr-LREE-As-Sb-Bi.

The eastern zone is distinctive because it appears to be mainly a replaced medium-coarse-grained amphibolite, within a tight D₂ fold adjacent to an unexposed east-west fault (Fig. 3). In outcrop it is represented by a 50 m long

Plate 1: (see page opposite)

- (a) MKD2/40m In situ tectonic breccias broadly related to boudinage, with pyrite-magnetite veining carbonate (rims) and biotite (centres) clasts;
- (b) peperitic amphibolite margin, displaying characteristic silicified sediments, and sediment clasts;
- (c) magnetite-infiltrated silicified mylonite, immediate ore hangingwall;
- (d) MKD1/64.7m Small boudinage neck vein in muscovite-quartz schist, with quartz fill, a fine garnet and pyrite selvage, brown carbonate alteration, and crack-filling magnetite;
- (e) Typical weathered Monakoff Western Zone ore, with a planar foliation, and pink barite-fluorite with black Mn staining;
- (f) MKD1/51.5m. Epidote alteration around thin quartz veins in amphibolite, hangingwall;
- (g) MKD1/78.0 m. Typical chalcopyrite-rich mineralisation, Monakoff Western Zone
- (h) MKD1/64.3m. Quartz vein-fill in a boudin-neck zone, with corresponding dark Mn-Fe-carbonate and magnetite metasomatism (dark laminae), fringed by biotite-garnet alteration;
- (i) MKD1/74.5m. (f.o.v. 2mm, crossed polars) sample at the biotite-garnet and carbonate-barite boundary, showing garnet-biotite breakdown.

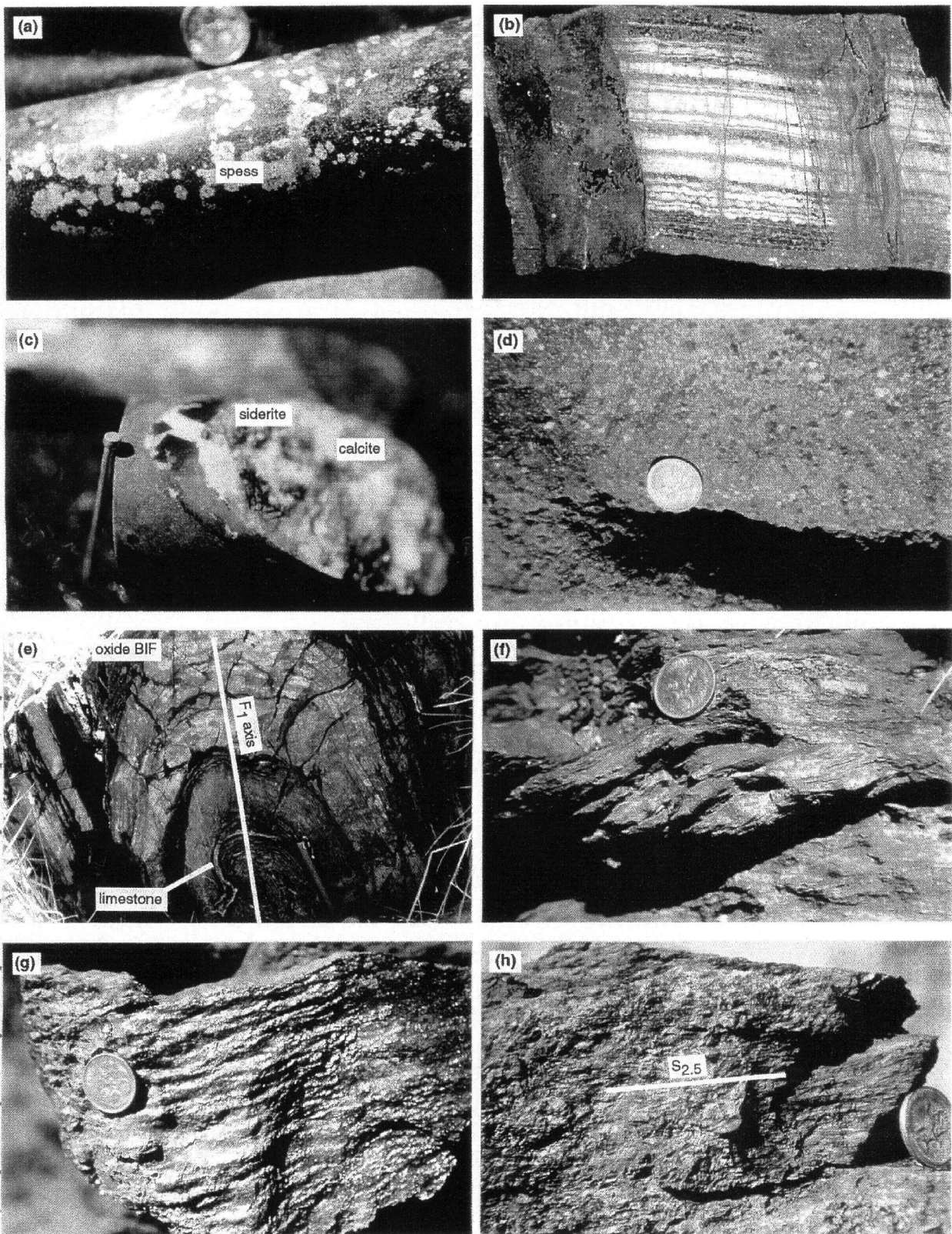


Plate 2:

- (a) MKD1/93.3m Typical porphyroblastic garnet-biotite schist, identified as a meta-dacite/andesite;
- (b) Banded iron formation from the “ore package”, transected by numerous coarse and fine weathered sulphide veins;
- (c) MKD1/115.7 m. Siderite (brown)-calcite vein (post-ore) with a magnetite-destructive halo in footwall porphyroblastic garnet-biotite schist;
- (d) Coarse magnetite-barite assemblage from the Monakoff Eastern Zone, representing altered coarse amphibolite;
- (e) F1 shallowly west-plunging isoclinal fold in carbonate and oxide iron formation, 4 km west of Monakoff;
- (f) Dextral shear indicator (looking straight down at vertical S1) in the Monakoff Shear, ~ 5175E; prospect grid;
- (g) D3 crenulations in massive biotite ore selvage (~5175E; not in situ);
- (h) F2.5 fine crenulations in chlorite-spessartine schist adjacent to ore (~5175E), viewed in situ looking north at a vertically dipping S1 surface.

hill edged by small cliffs. This hill consists of buff silica, studded with randomly oriented crystals of coarse magnetite, magnetite-hematite, and hematite, that are unlike any fabric in the western zone, and are consistent with faithful pseudomorphing of meta-gabbro (Plate 2d). The silica may be a surficial replacement product of carbonate, since silica is not abundant in the ore at depth here. The hill occurs within a steeply west-plunging fold structure defined by bedding trends in banded iron formation and metasediment. 100 m west along strike, drill hole MKD2 indicates that the less altered equivalents of the folded package are comparatively thin massive meta-dolerites and intercalated peperitised sediments. The meta-dolerite/sediment contacts are preferentially silicified in MKD2, with an alteration zonation into the sediment of siderite-magnetite-pyrrhotite-chalcopyrite, magnetite-siderite-quartz, to biotite-quartz-magnetite over 1 m or less. The adjacent dolerite contains incipient siderite alteration. It is interpreted that in the core of the fold, severe alteration affected the interior of the folded metadolerite as well as the sediment margins, with fluids tightly focussed by the fold structure, resulting in wholesale replacement of dolerite. This produced a narrow west-plunging pipe with Cu grades of 1.4-3.0%, consisting of siderite-barite-magnetite-chalcopyrite, which is likely to have considerable depth extent. The fold-hinge control, the transgressive character, and dolerite host-rock all indicate that the Monakoff East Zone developed during deformation, rather than before it.

In addition to the two main ore zones, minor mineralisation occurs on many steeply dipping contacts within both the footwall and hangingwall sequence, although mainly in the footwall. In particular, amphibolite-sediment contacts display mineralisation, with local alteration haloes in each lithology. This is evidence that steeply dipping contacts were dilational during ore formation not only on the main shear zone, but also generally in the host-sequence, at least 200 m into the footwall. The early silicification (pre-ore) which preferentially characterises amphibolite contacts, is fractured, and commonly contains disseminated siderite-magnetite-pyrrhotite-chalcopyrite, grading out to disseminated magnetite-siderite, and then to biotite-magnetite over 0.5–2.0 m (eg., from 114.0 to 119.2 m, in MKD2), probably resulting from local gradients in the activity of S and CO₂.

Alteration and Ore Mineralogy

The following alteration zones are recognised around the Monakoff Western Zone, and are summarised in Fig. 4:

Weakly Altered Host Rock

Meta-siltstone constitutes the immediate ore hangingwall and footwall. It consists of 1-3 mm wide segregated bands of alternating phyllosilicate and quartz-dominated assemblages. In detail each assemblage consists of: 1). muscovite-biotite-garnet-magnetite-quartz±chlorite, and 2). quartz-albite±magnetite (some albite grains are much

coarser than the deformed quartz matrix, up to 200 μm, which is consistent with a local immature feldspar sediment source). 1-3 cm scale folds (F3) defined by banding, in detail contain an earlier muscovite-defined differentiation schistosity, crenulated by a second muscovite-defined cleavage (S2/S1). Thin (250 μm) veins of recrystallised quartz-magnetite-pyrite-chalcopyrite are sub-parallel to S1/S2, but are folded by S3. Chalcopyrite was invariably formed by replacement of some coarser magnetite. Garnet (white, euhedral; 100–200 μm diameter), does not contain any inclusion-defined cleavage, leading to the conclusion that at least some garnet grew prior to S2. As a possible distal ore halo within 10 m of mineralisation, and as small halos to isolated zones of epigenetic mineralisation, a second garnet generation overgrew the widely distributed garnet porphyroblasts: the overgrowths are a white, birefringent, uvarovitic variety. The overgrowths do not show substantial pressure shadowing even where quartz in the same rock displays large grain-preferred aspect ratios parallel to the muscovite-defined cleavage. Biotite defines a separate cleavage at ~15° to the main muscovite cleavage (S2), and preferentially forms fine lenses that in hand-specimen impart a dark flecked appearance. It is not possible to say whether this is S2.5 or S3. A second foliated biotite generation occurs with spessartine in a proximal alteration shell, and a third occurs as isolated, ragged, disoriented brown biotite throughout the prospect. On the basis of very strong pressure-shadowing around magnetite-carbonate intergrowths, some small magnetite and carbonate porphyroblasts grew prior to S1/S2, whereas the location and orientation of most other carbonate porphyroblasts is controlled by the crests of S2.5 crenulations, and quartz within the porphyroblasts is crenulated by S2.5 (eg., in MKD1 at 66.4 m). This indicates that most carbonate was introduced during or post S2.5 development.

Alteration Associated with Local Boudinage

Oblique boudinage zones occur both in the weakly altered and main alteration zones, and are surrounded by distinct small metasomatic haloes that provide information on the timing of general mineralisation. These boudinage zones vary in scale from a few centimetres to >5 m in scale, and are also gradational to fracture networks. The metasomatic haloes around boudinage neck veins are similar to those that characterise small mylonitic breccias in the hanging wall, and appear to be sites where more proximal alteration types are favoured, particularly massive magnetite metasomatism (Plate 1h). Veins are zoned from an internal fill of quartz-sphalerite-galena-pyrite-carbonate (quartz is strongly undulose, with serrated grain boundaries), with pink garnet edges, to an immediate wallrock alteration zone of fine pink euhedral garnet+magnetite, both embayed by carbonate. Garnet is cracked and altered by chalcopyrite (Plate 3b) and fibrous stilpnomelane in radiating aggregates immediately adjacent to veins, where it also shows maximum replacement by carbonate. Pyrite within veins is replaced by dolomite rhombs along fractures. Magnetite occurs both as intense replacement along and around fractures adjacent to veins, and as disseminated crystals

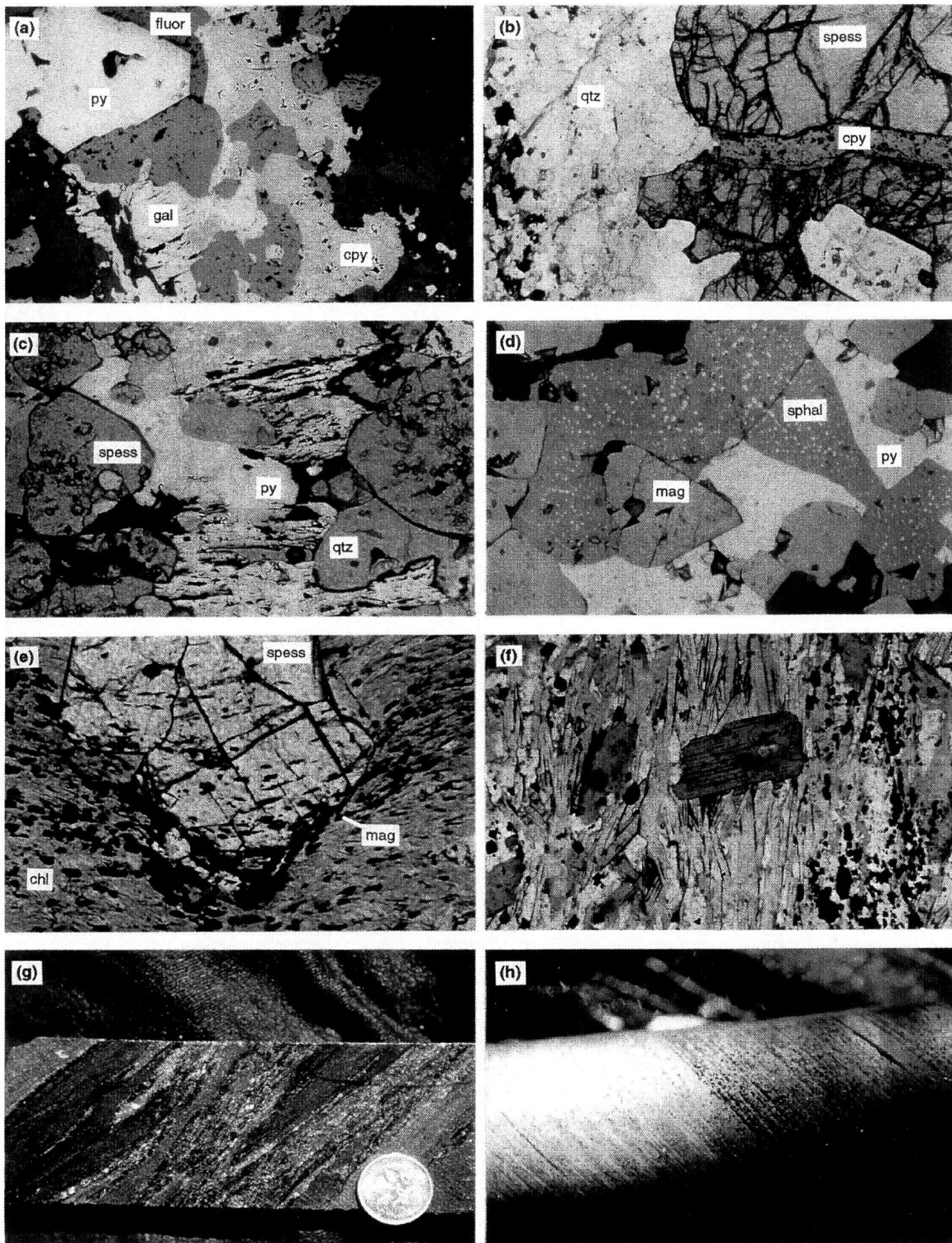


Plate 3:

- (a) MKD1/78.2m Reflected light of typical ore relationships, galena distributed around the margins of a fluorite grain, which is in contact with euhedral pyrite;
- (b) MKD1/93.3m (f.o.v. 2mm; transmitted and reflected light) Spessartine with a quartz halo in the garnet-bearing footwall, cut by a chalcopyrite-chlorite vein, filling fractures;
- (c) MKD1/87.0m chalcopyrite-garnet replacing an antecedent cleavage;
- (d) MKD1/79.0m (f.o.v. 1mm; reflected light) Euhedral to subhedral magnetite overgrowing chalcopyrite riddled sphalerite, and pyrite;
- (e) MKD1/71.8m (f.o.v. 1mm) Chlorite and garnet overgrowth of a D2.5 crenulation that is defined by elongate magnetite foliation, with post-crenulation magnetite concentrating around the garnet; (f) MKD1/74.5m (f.o.v. 0.5mm) biotite-garnet alteration used for garnet-biotite geothermometry, illustrating the dominant early biotite fabric (syn-D2.5), overgrown by younger disoriented biotite, a typical feature of the whole area;
- (g) MKD2/58.5m Near-foliation parallel fractures infilled by carbonate-barite ore, with the clasts consisting of fine-grained precursor magnetite-quartz;
- (h) MKD2/ 170m. Fine tectonic/sedimentary compositional lamination with small dark biotite concentrations in the foliation, shear zone adjacent to the Monakoff eastern Zone, Mt Norna Quartzite.

throughout the host rock. Chalcopyrite is not an obvious vein fill, but instead replaces magnetite, garnet and carbonate along fractures (Plate 3b).

Chlorite-Garnet Alteration

The main minerals in this zone are chlorite, plagioclase, garnet (3 growth phases described earlier), 2 biotite generations, carbonate and sphalerite. Compared to the weakly altered host rock, fine euhedral isotropic garnet is mainly absent, but minor granular relics on the edges of carbonate lenses are evidence of its former presence. Chlorite is foliated and also crenulated (Plate 3e), and replaces foliated biotite, which is commonly only present as slight brown streaks in the chlorite (eg., in drill hole MKD1 at 71.8 m). Garnet (pink spessartine) and chlorite appear to have been in metamorphic equilibrium. Garnet however, where in contact with carbonate, is embayed and granulated (Plate 11). In terms of timing, it is not clear whether chlorite overgrew or was foliated by S2. As noted earlier, garnet preserves a crenulated quartz inclusion-defined foliation, consequently, most garnet grew syn- to post-S2.5. Elongate relict subhedral plagioclase defines a cleavage (S1), which is crenulated by the chloritised biotite cleavage (S2), forming a weak segregation cleavage relationship.

Biotite-Garnet Alteration

The transition inward to biotite -garnet \pm plagioclase-magnetite assemblages is gradational over 10 cm, forming a massive foliated rock dominated by biotite (Plate 2g). Inward, some biotite-garnet to carbonate-quartz metasomatic contacts preferentially contain sphalerite disseminated immediately within the carbonate-quartz zone, and fine pink garnet concentrated close to the contact within the biotite zone. Biotite defines two moderate cleavages (an early cleavage, and a second crenulating cleavage at a small angle to the first), but is more randomly crystallised than adjacent relict host-rock muscovite. There is minor evidence of a second randomly oriented third biotite generation (Plate 3f). Garnet contains randomly-oriented inclusions of plagioclase rather than a foliation, has pronounced pressure shadows of carbonate-quartz \pm magnetite, and also distorted biotite around its margins, suggesting that some garnet cores grew prior to S1/S2, growing in the prograde metamorphic episode prior to S1 (O'Dea et al., 1997). This conclusion is based upon the principle that garnet will always preserve a pre-existing foliation. Consequently, there is evidence of early garnet, syn-metasomatic garnet (Syn-D2.5), and post-D3 garnet overgrowths in this part of the Monakoff shear zone, and the textural difference between them is not as clear as in outer alteration zones. Magnetite is concentrated around the margins of garnet (Plate 3e) and follows distortions in the biotite schistosity, indicating that it grew syn- to post-biotite. Magnetite is notably absent in the carbonate-quartz zone. Propagation of the metasomatic zonation occurred preferentially along small ductile faults (plate 3g). Here

micro-zonation occurs inward from biotite \pm sphalerite, to carbonate-quartz-garnet-biotite (in which garnet displays severe breakdown to carbonate), inwards to quartz-only, with minor relic biotite grains remaining on the triple point margins of recrystallised quartz.

Carbonate-Quartz/Barite-Carbonate Ore Zones

In the contact transition between metasomatic zones, several of the macroscopically identified assemblages may occur in close proximity in foliation-sub-parallel breccias. These include multiple planar low-angle metasomatised faults and fractures in which breaks contain barite-carbonate alteration around clasts of biotite-plagioclase \pm disseminated magnetite, with carbonated rims, or alternatively biotite-altered rims and carbonated cores. Beyond the contact zones in massive ore, there is a general antipathetic relationship between sulphides and magnetite. A compressed broader alteration zonation can occur over 5-10 cm in this contact region, with for instance, a transition from biotite-plagioclase, to coarse garnet (with evidence of carbonate replacement), to massive carbonate, to carbonate-quartz-barite-chalcopyrite-pyrite. Minor phases in the carbonate-barite zone include: 1). monazite on contacts between biotite and quartz; 2). epidote in places displaying replacement by carbonate; 3). fluorite occurring as ovoid inclusions within quartz and carbonate; and 4). hematite occurring as $<1-5 \mu\text{m}$ inclusions along barite grain boundaries with carbonate. Fluorite and coarse magnetite are enriched in the centres of ore intersections (Fig. 4).

The barite-carbonate zone does not contain definitive timing criteria to assist correlation with external deformation events. It possesses a granofelsic texture, with only a moderate cleavage in the adjacent biotite 2 zones. Crude petrographic timing evidence for ore includes: 1). overgrowth of foliation by unfoliated chalcopyrite; and 2). replacement of spessartine in porphyroblastic garnet-biotite schist by chalcopyrite along veins and fractures. There is evidence of magnetite breakdown to form sulphides, indicating that magnetite is paragenetically earlier than most sulphide. The evidence consists of an antipathetic relationship between the two, the occurrence of magnetite inclusions in euhedral coarse pyrite crystals, and a general highly amoeboid grain habit for magnetite, compared to its euhedral habit in adjacent zones. This occurs in both Monakoff East and West zones. Barite commonly does not contain any magnetite inclusions and only rare sulphide inclusions, but chalcopyrite and pyrite inclusions are commonly present in magnetite. However, in the central high-grade sections of ore intervals, coarse magnetite is stable in contact with pyrite, sphalerite and galena. This inherent paragenetic contradiction for magnetite over short intervals could be explained if the coarse magnetite described here, and mapped in the Monakoff Eastern Zone at surface, is metamorphic, and like some biotite in the surrounding alteration, was produced by a thermal event following the main ore event.

Summary

The following metasomatic paragenesis is observed:

Pre-ore - Epidote alteration of mafic sill margins, and silicification of mafic sill sediment contacts. K-Fe-Mn alteration of meta-andesite, which recrystallised to spessartine-biotite-chloritoid during pre-D1 metamorphism;

Stage 1 - Biotite-magnetite alteration, focussed upon a D1 shear zone;

Stage 2 - Chlorite-garnet/biotite-garnet/carbonate-fluorite-barite zonation (ore formation);

Stage 3 - "Mt Freda"-style ferro-carbonate veining and minor breccia, with haloes of sericitisation in amphibolites; and

Stage 4 - Pervasive albitisation focussed along NW oriented faults.

Stage 1 was an early post-D2 event in which fine-grained biotite pseudomorphed 2 muscovite-defined cleavages. Stage 2 was timed closely to D2.5, which overprinted the more extensive but disseminated Stage 1 assemblage. Given that brecciation and well-developed mineralisation coincide with higher magnetite concentrations, it is possible that the earlier phase, which produced variable abundances of fine-grained magnetite, partly controlled the location of ore development in the later phase. However, primary magnetite concentrations, such as the persistent BIF horizon

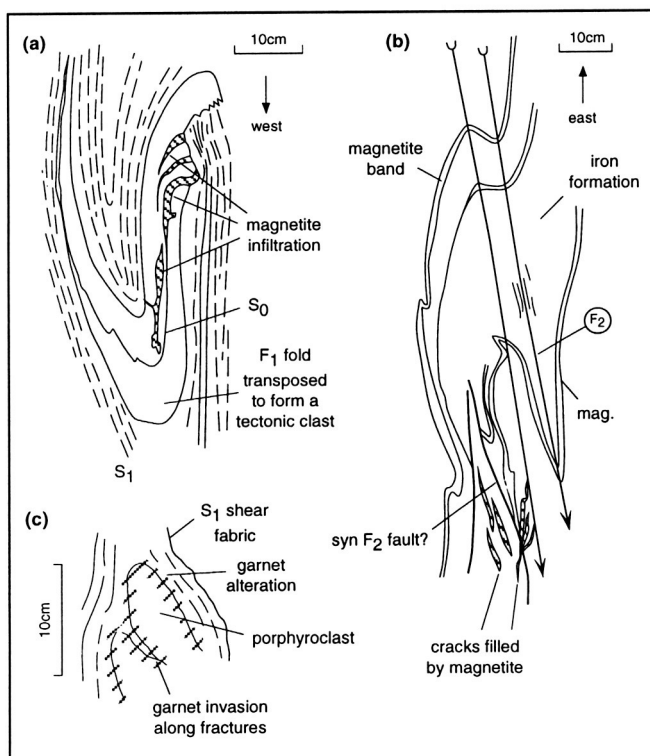


Figure 5: Plan views at varying scales of:

- an F1 dismembered fold-hinge with preserved magnetite infiltration around the clast margins;
- a typical small-scale F2 fold plunging steeply west, emphasising the variable effect of F2 on adjacent lithologies;
- garnet metasomatism around a tectonic clast within the Monakoff Shear.

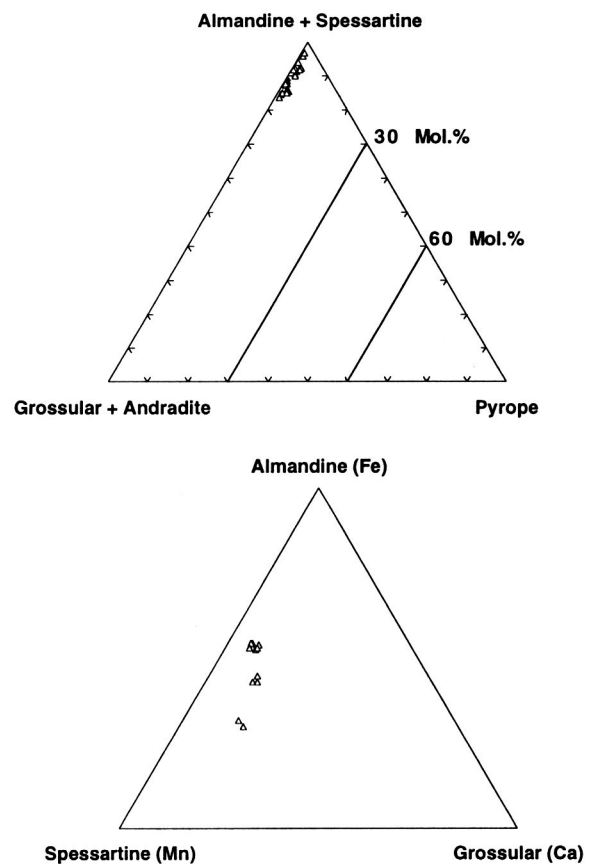


Figure 6: Monakoff garnet compositions

in the footwall package, experienced metasomatism and moderate infiltration by barite-forming fluids, but were not severely replaced. Consequently magnetite was an important but not vital prerequisite for ore formation. The solution to this contradiction may lie in the location of the main shear zone relative to magnetite concentrations, with zones of shear-hosted magnetite being subject to greater extension, permitting greater fluid access during the ore event.

Mineral Chemistry

8 thin-sections were analysed across the Monakoff Western Zone from drill hole MKD1 from 66.3 to 93.3 m, targeting biotite, garnet, chlorite, carbonate and sundry phases, with the aim of: 1). characterising the compositions of the important alteration phases; 2). determining whether mineral chemistry is a more effective tool than whole rock geochemistry for exploration for Monakoff-style targets; and 3). to determine if there is a significant compositional difference between pre-metamorphic and metamorphic alteration. Analyses were obtained with an SX50 Cameca microprobe running at 15kV and 10 nA.

Garnet

Garnets divided into low Ca-Mg spessartines and Mn-almandine varieties, with $X_{\text{spess}} = 0.23\text{--}0.58$ (Fig. 6). A typical metasomatic garnet has a composition of $\text{Py}_{0.00}\text{Alm}_{0.47}\text{Gro}_{0.06}\text{Spess}_{0.47}$. The porphyroblastic garnets of the altered meta-dacitic footwall contain lower Mn

contents ($X_{\text{spess}} = 0.23\text{--}0.35$) than garnets in the ore halo. Rim contents of some garnets vary significantly (are more Fe-rich) from core compositions in some samples, particularly where distinct garnet overgrowths occur (Mn content in garnet increases through the metasomatic halo towards the ore zone, and is highest in the biotite-garnet zone. However, even weakly altered schist garnets contain 15–20 wt.% MnO (Fig. 7). The lower garnet Mn values in footwall schist are consistent with the observed whole-rock Mn decrease away from ore.

Biotite

Biotite compositions are very variable, with $(\text{Mg}+\text{Mn})/(\text{Mg} + \text{Mn} + \text{Fe})$ ratios of 0.1–0.65, and octahedral aluminium values of 0.03–1.16. Consequently they cover most of the solid solution between annite and siderophyllite varieties. They possess high F and low Cl contents, typically F ~2 wt.% [maximum 3.12 wt.%] and Cl ~ 0.02–0.2 wt% in ore, with cation F/Cl ratios of 20–200 adjacent to the ore zone, grading to 0.5–20 in the peripheral weakly altered areas, where F descends to 0.5–0.8 wt.%. The physical variation of F in biotite across the Monakoff Western Zone closely mimics Mn variation in garnet - F is elevated in weakly altered muscovite-garnet schist, is highest in the biotite-garnet zone adjacent to ore, and lowest in foliated biotites of the porphyroblastic garnet-biotite footwall. A clear control on F is the Mg content of biotite, itself a function of metamorphic conditions. F is strongly positively correlated with Mg, which is an expression of the well-documented ‘Fe-avoidance’ rule for F in mica and amphiboles (Munoz, 1984).

Carbonate

Carbonates have not been extensively analysed, but carbonate spotting in the biotite-garnet alteration consists of manganoan calcite, which is typically $(\text{Ca}_{0.87}\text{Mg}_{0.02}\text{Mn}_{0.07}\text{Fe}_{0.03})\text{CO}_3$, with Mn varying from 6 to 7 wt. % in a slide, whereas the adjacent carbonate-barite mineralisation contains iron-rich rhodochrosite, known as the variety ‘ponite’ (Deer et al., 1992), defined as rhodochrosite with up to 20 wt. % Fe. The ore carbonate has a typical composition of $(\text{Ca}_{0.07}\text{Mg}_{0.04}\text{Mn}_{0.6}\text{Fe}_{0.29})\text{CO}_3$. This follows the behaviour of ore elements in other phases as the ore conduit is approached, with very large increases occurring over a short distance.

Whole Rock Geochemistry

Methods and Results

Samples were selected regularly across the mineralised zones in three separate diamond drill holes, with representative samples of adjacent lithologies also taken for comparison. The aim of this work was to: 1). characterise the composition of alteration and ore; 2). identify any important trends in the alteration geochemistry away from ore; and 3). identify elemental relationships that constrain genetic models for Monakoff. Samples were processed at James Cook University, and analysed both by XRF and neutron activation. A comparison of results of the exploration data for Cu, taken at 1 m intervals, compared to samples taken by this study (30 cm sticks of quarter- to half-core at 1–5 m intervals)

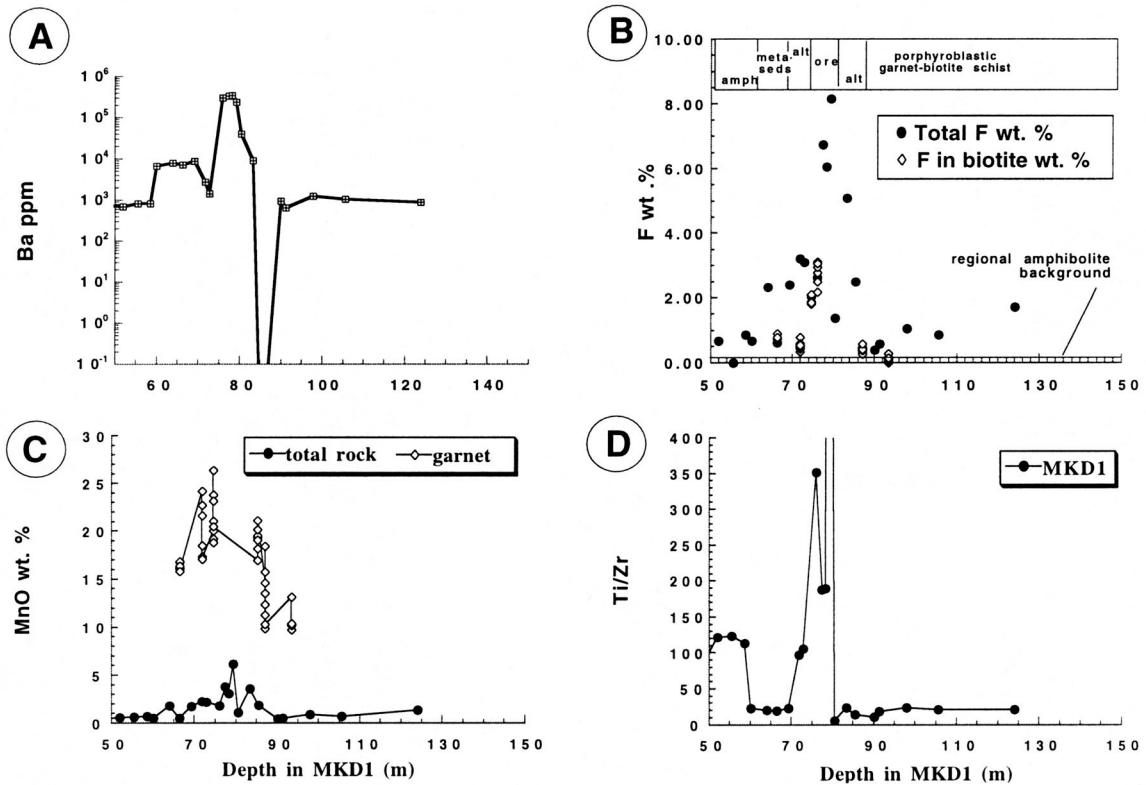


Figure 7: Downhole geochemical profiles in MKD1 for:

- (A) Ba; (B) F, including trends in mineral chemistry biotite;
 (C) MnO including garnet composition trends; (D) Ti/Zr.

	MKD1/7 6.0m	MKD 1/77.4m	MKD1/ 78.2m	MKD1/7 9.3m	MKD1/49. 8m	MKD1/6 4m	MKD1/66. 3m	MKD1/72. 8m	MKD1/12 4m
	Ore	Ore	Ore	Ore	Weakly altered amphib	Host musc schist	Stage 1 biotite alteration	Stage 2 chlorite- garnet	footwall garnet- biotite
SiO₂	9.29	0.59	0.45	1.33	47.93	56.32	59.74	42.48	61.17
TiO₂	0.15	0.11	0.11	0.08	0.99	0.61	0.67	1.07	1.02
Al₂O₃	2.28	0.79	0.79	0.71	14.43	15.44	16.92	13.30	12.64
Fe₂O₃T	12.84	15.01	15.38	23.27	13.37	14.10	11.67	13.01	13.62
MnO	1.82	3.76	3.05	6.13	0.51	1.79	0.54	2.22	1.33
MgO	0.43	0.39	0.35	0.49	8.29	1.32	1.10	5.05	0.55
CaO	11.97	11.99	12.48	9.55	9.61	2.09	0.73	9.26	3.01
Na₂O	0.00	0.00	0.00	0.00	2.69	0.28	0.38	2.42	3.12
K₂O	0.62	0.00	0.03	0.04	0.54	4.56	5.31	0.40	2.04
P₂O₅	0.35	0.25	0.26	0.17	0.07	0.59	0.18	0.09	0.29
S	22.05	22.85	23.20	21.46	0.09	0.14	0.19	0.55	0.02
F	2.62	6.74	6.06	8.16	0.59	2.33	0.62	3.10	1.72
BaO	30.75	34.36	34.79	26.40					
CuO	4.08	2.70	2.81	1.91					
L.O.I	0.00	0.63	0.00	1.63	1.40	2.11	1.93	7.90	1.60
minusO=F	1.10	2.83	2.54	3.43	0.25	0.98	0.26	1.30	0.72
SUM	97.23	96.46	96.08	96.85	100.35	101.58	100.54	99.67	101.47
<i>Ag</i>	72.50	63.70	71.30	-20.00					
<i>As</i>	2010	2350	2280	1360	8.59	53.9	7.1	6.12	2.02
<i>Au ppb</i>	699	795	665	481					
<i>Ba</i>	303000	336000	352000	239000	726	7800	7170	1410	873.00
<i>Cs</i>					4.93	13.1	9.46	5.57	6.30
<i>Co</i>	1260	1670	1700	1490	56.2	44.2	10.4	52.7	11.20
<i>Cu</i>					189.4	8872.6	31.2	937.5	58.10
<i>Ga *</i>	2.40	0.00	6.30	7.10	19	21.1	28.6	15	19.90
<i>Hf</i>	5.34	3.58	5.09	2.64	1.3	90.1	4.98	1.64	8.07
<i>Ir ppb</i>	-20.00	-20.00	-20.00	-20.00					
<i>Mo</i>	-500	-400	-500	-200					
<i>Nb *</i>	0.00	0.00	0.00	0.00	3.6	0	1.1	2.5	17.80
<i>Ni *</i>	41.10	51.90	50.10	37.10	124.1	36.9	34.8	113.3	8.20
<i>Pb *</i>	2694	3210	5076	5998	21.1	12.2	11.2	79.4	7.00
<i>Rb *</i>	10.70	0.00	0.00	0.00	45.2	333	353	35.5	97.70
<i>Sb</i>	402	226	120	24.70	2.4	1.52	0.93	1.87	-0.20
<i>Sc</i>	2.01	0.44	0.48	0.56	39.7	13.7	14.7	38.7	20.70
<i>Sr *</i>	66701	10675	8406	5089	221.3	112.1	65	163.6	45.70
<i>Ta</i>	-2.00	-2.00	-2.00	-1.00	1.04	1.24	2.01	-1	2.09
<i>Th</i>	3.41	3.85	-1.00	1.75	0.74	17.2	18.7	1.08	10.90
<i>U</i>	334	284	307	164	-2	10	-2	-2	-2.00
<i>V</i>					275.2	106.2	69	292.5	16.30
<i>W</i>	80.90	150.00	151.00	169.00	44.3	16.1	7.76	-4	-4.00
<i>Y</i>					18.3	21	23	14.6	54.20
<i>Zn</i>	7060	10300	10900	9540	465	262	176	3300	139.00
<i>Zr *</i>	1.00	1.00	1.00	1.00	55.2	170.7	194.7	66.8	319.20
Ce	1150	880	920	436	9.34	105	104	30	57.50
Eu	6.72	4.64	5.83	4.44	0.79	1.57	1.51	0.56	2.12
La	1680	1420	1470	753	3.96	67.5	56.5	25	27.80
Sm	6.95	6.22	6.15	4.13	2.31	7.88	8.14	3.2	8.60
Tb	1.09	0.85	0.90	0.63	0.53	1.02	1.13	0.52	1.77
Yb	0.53	0.50	0.50	-0.50	1.59	2.71	3.03	1.65	6.45

Table 1: Typical composition of ore zones and host rocks in diamond drill hole MKD1.

* indicates XRF data, with all other data derived by neutron activation;

Detection Limit numbers only apply to neutron activation data;

Negative indicates "less than" in neutron activation data.

Sn was measured at 0.0 in all ore samples.

were surprisingly different, and indicate that the research sampling, although detailed, does not provide as accurate a guide to elemental distribution as the exploration sampling (Fig. 8). Typical analyses are presented in Table 1.

Ores

Monakoff ores are geochemically very complex, although their major components (>10 wt.% oxide) are, in order: S, Ba, F, Fe and Ca, with the significant minor element enrichments including (* denotes elements at economic concentration) Sb, As, Co*, Cu*, Au*, Pb, Ag*, W, U, La, Ce and Zn, as well as an astonishing Sr abundance (Sr = 0.5-1%; highest recorded value of 1.07 wt.%). Mo and Sn are high in surface samples (Davidson, 1994), but detection limits by neutron activation were a problem for these elements. Other elements with high neutron activation detection limits that have not been adequately characterised are Ir, Br, Ce, and Se. Considering the previous comparisons between Monakoff and BHT-style Pb-Zn systems (Ashley, 1983; Derrick, 1996), P₂O₅ abundances are surprisingly low, with most ores containing only 0.2–0.4 wt.% P₂O₅. The highest values were systematically found in the iron formation, although several high Fe samples in the immediate ore halo in Monakoff Eastern Zone possess values of up to 1.88 wt.%. However, no strong Fe-P correlation exists when all the data is considered. La and Ce abundances are also very high, with typical values of >1000 ppm. Rather than apatite, the host phase for REE, U, and possibly P₂O₅, is monazite, which is common in

ore intersections (see petrography), and concentrates the LREE. Zr is unusually low, 1–5 ppm.

Host Rocks

The broad physical patterns of geochemical behaviour of the host rocks are reviewed herein. The three major lithologies (amphibolite, footwall porphyroblastic garnet-biotite schist, and meta-pelite) all have distinctive Ti/Zr ratios (Fig. 7) unless they are visibly altered, at which point Ti/Zr is disturbed. The alteration and ore Ti/Zr signature is very high (>100), but the uncertainty caused by Sr interference with XRF Zr remains a problem (see above). Of the elements found to be enriched in ore, Mn and F have the most consistent regional distribution in the associated alteration, and F is particularly interesting in terms of exploration potential because of the low F background in normal crustal rocks. Mn in the alteration is consistently >2 wt% MnO, but the whole sequence has a high Mn background >0.5 wt.%, compared to the regional amphibolite MnO background of 0.15-0.30 wt.% (Unpublished AGSO geochemical database). As previously discussed, on the basis of textures, this Mn enrichment is considered to at least partly relate to a pre-metamorphic hydrothermal alteration event (Ashley, 1983).

Less ambiguously, F is >0.5 wt.% over the entire 132 m length of MKD1, a drill hole that terminates in footwall garnet-biotite schist. The enrichment occurs in footwall garnet schist, the alteration and ore, and the hangingwall

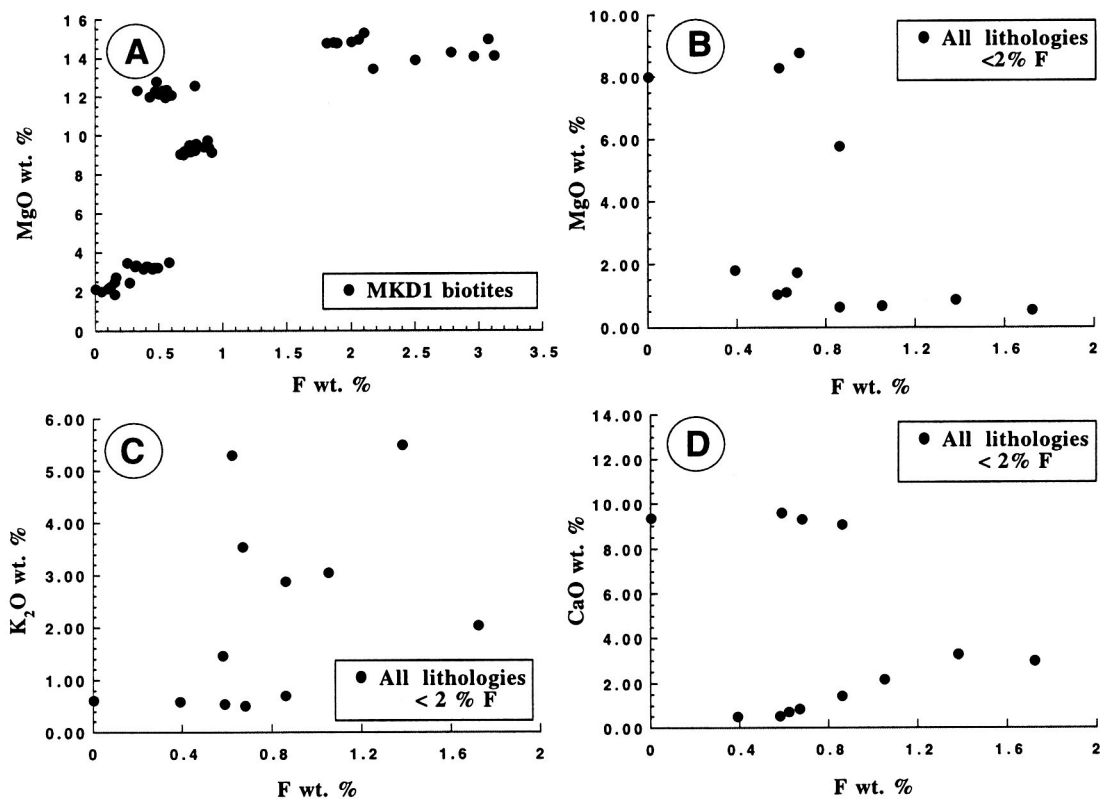


Figure 8: Relationships between F and other major elements for all lithologies in drill hole MKD1, including (A) the mineral chemistry of biotite; (B) MgO; (C) K₂O; (D) CaO.

These elements were plotted to evaluate the behaviour of F compared to fluorite and biotite variation.

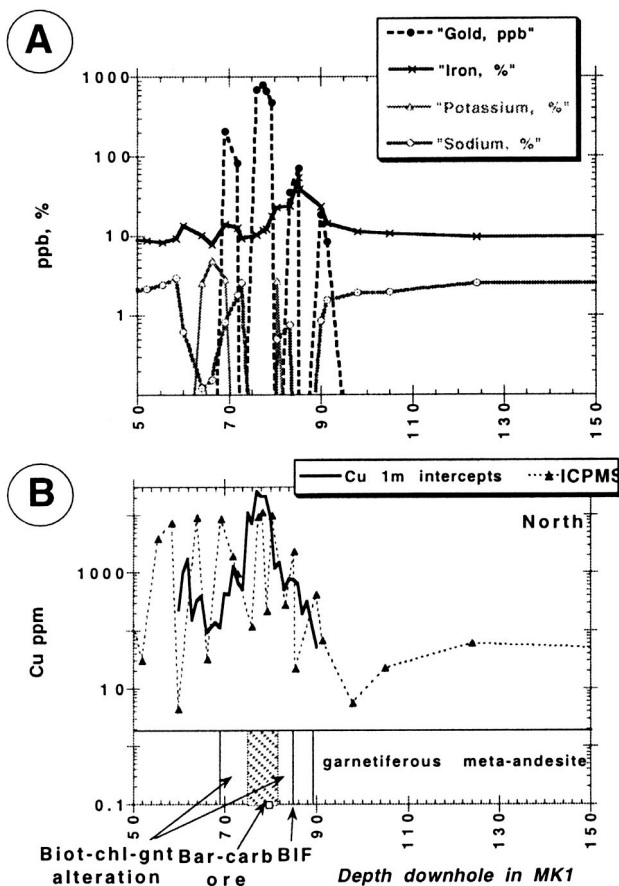


Figure 9:

- (A) Downhole behaviour of Au, Fe, K, Na, and Cu in MKD1
 (B) Cu behaviour, at >1 m sampling intervals, by ICPMS, in this study, compared to 1 m intercepts data obtained by Esso Minerals (Ashley, 1983) by atomic absorption.

amphibolites. Regional Toole Creek Volcanic amphibolites contain F <200-500 ppm. In MKD2, the Monakoff F halo terminates sharply at the base of the garnet schist, dropping to background (200 ppm F; unpublished AGSO geochemical database) within the metasediment (Fig. 10), a behaviour that is closely mirrored by Mn. The F enrichment has great potential as an exploration indicator, because it enlarges the ore halo by >10X the width of the visible alteration zone. The control on fluorine enrichment has already been examined mineralogically, where the Fe-avoidance rule was shown to be operating for Monakoff alteration biotite, and presumably also for other hydrous phases. However, plots of potential element correlations, such as K as a measure of biotite enrichment, or Ca as a measure of available Ca for fluorite precipitation, do not show any coherent co-variation with F (Fig. 8). High background F concentrations may therefore be caused by substitution into several different phases with different major element compositions, rather than into a single phase. There is nevertheless a clear enrichment in igneous over sedimentary lithologies which is not yet understood.

Ore elements U, Zn and Ba all also have large haloes (Fig. 11), although not as extensive as F. There is no definite zoning in the ore elements through the alteration, with U, Zn, Ba and Cu all displaying similar peaks through the

MKD1 ore zone, dropping off into the alteration in a symmetric fashion, with the exception of Ba, which is enriched in hangingwall alteration relative to footwall (Fig. 11). These elements display positive linear co-variation with F, which is consistent with F-metal complexing. However, simple co-precipitation of phases can also produce similar geochemical behaviour on binary plots, as demonstrated for Ba (Fig. 11), so that fluorine complexing is likely but not proven.

Fluid Inclusions

Workable fluid inclusions are not abundant in the Monakoff replacement ores, but are present in minor quantities in some boudin neck veins, such as found in drill hole MKD1 at 60.8 m (Quartz-garnet-pyrite-sphalerite-galena in boudinage fill). No heating and freezing data are reported here, but the veins have the following inclusion populations:

Type 1. Primary inclusions: 5-15 μm vapour-only and L-V inclusions, with strong negative crystal forms, occur in patches in quartz and garnet. Those in garnet are round-edged circular- to pear-shaped 5-40 μm inclusions arranged centripetally around growth zones, with variable liquid-vapour ratios, from ~20% liquid, up to nearly 100%, and no daughter salts. The liquid-rich examples have complex decoration within the inclusions, whereas the vapour-rich examples have negative crystal shapes. These inclusions are additionally most pronounced where they are completely surrounded by a sulphide phase. Similar examples in open areas of quartz are collapsed and emptied, consistent with destruction during subsequent deformation.

Type 2. Secondary or pseudo-secondary inclusions: 5-25 μm square liquid-dominated inclusions with 5-10% vapour by volume, and two isotropic square daughter salts (probably halite and sylvite). Inclusions occur in patches in quartz, in close proximity to sulphide inclusions, and also in continuous planes.

Type 3. Secondary or pseudo-secondary inclusions: 2-15 μm square liquid-dominated inclusions with 5% vapour by volume, and no daughter salts. Inclusions occur in planes in quartz, but are not related to quartz grain boundaries.

The primary inclusion types correspond most closely with liquid-dominated type 2 inclusions of Dong (1996), which she regionally correlates through a wide variety of Cu-Au deposits. Dong (1996) type 2 inclusions occur with mineralisation. The variable L-V ratio of inclusions in Monakoff boudin necks can be accounted for by: 1). fluid mixing; 2). boiling; or 3). condensation.

Discussion

The most detailed previous ore genesis model (Ashley, 1983) envisaged 'stratiform polymetallic ore' to have formed in 'a marine environment at a time when conditions were changing from possible turbidite sedimentation to a

major pulse of mafic magmatism'. Exhalation at this time 'precipitated chemical sediments of iron formation which were commonly rich in base metals, Ba, S, F and Mn, as well as containing highly anomalous values of U, REE and chalcophile pathfinder elements'. These views were supported by Derrick (1996), who described the ore as 'layered granoblastic exhalite containing barite-Mn carbonate-garnet-quartz-magnetite-fluorite-pyrite-chalcopyrite'. Conversely, Laing (1991, 1998) interpreted the deposit as a replaced D1 mylonite, localised at the intersection of a later structure, although he concluded that the iron formation also had a structural-replacement origin. Davidson and Large (1998) included the deposit in an 'Iron formation associated' sub-class within the iron-oxide Cu-Au deposits of Australia, ascribing an epigenetic origin to the ore.

The following deposit features require an epigenetic origin for the ore and most associated alteration:

- 1) Symmetric shells of high temperature alteration around the mineralisation;
- 2) Textural evidence of pervasive replacement of a D1 mylonite fabric by ore, and the exploitation of structural fabrics by alteration:

- 3) Specific growth of ore alteration carbonates and garnets during D2.5 deformation;
- 4) Common boudinage neck zones containing the ore assemblages; and
- 5) The pipe-like geometry of the Monakoff Eastern Zone within a replaced D2 antiform, in detail texturally replacing coarse-grained amphibolite.

However, no evidence could be found to support the view of Laing (1991) that the underlying iron formation was also epigenetic in origin, although its high metal contents in places indicate that it participated in the ore event. It is extremely continuous at regional scales, is folded by D1 folds adjacent to the prospect area, exhibits anomalous box-fold geometries indicative of a distinctive rheological response to deformation, shows no association with the boudinage that is common in the ore package, and is well banded, with banding defined by alternating magnetite and quartz dominated layers. Detailed mapping shows that it is never the locus of the main mineralisation at either lens within the deposit, so that description of the deposit as 'iron formation associated' is misleading in the connotation that iron formation hosts ore; it does not. Fe-K-Mn alteration of the interpreted footwall meta-andesite is an asymmetric feature of the ore site. Here, spessartine, almandine garnet,

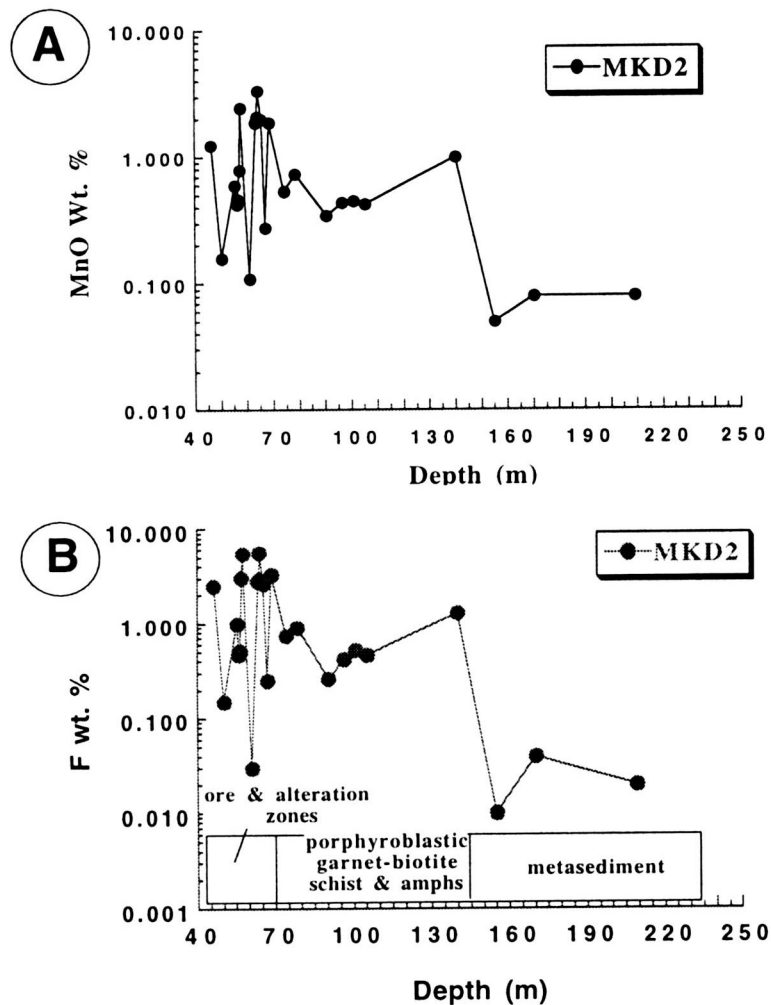


Figure 10: Downhole behaviour of (A) Mn; and (B) F in MKD2.

The northern edge of the F anomaly occurs at the meta-andesite/sediment boundary; this is the only hole in which the fluorine anomaly is fully defined in the footwall.

biotite and chloritoid occur pervasively within a thick massive rock mass. The random orientation of chloritoid could be accounted for by post-deformational growth. However, this observation, combined with the lack of foliation overgrowth by spessartine in this unit (in contrast to spessartine within the shear), and the overgrowth of spessartine by peak metamorphic almandine, forms a mass of evidence favouring development of the main mineral assemblage prior to foliation formation. Biotite orientation is controlled by several separate cleavages, and while it likely crystallised during pre-deformational metamorphism, there is little evidence of this now. It is concluded that an early hydrothermal history influenced the bulk geochemical character of the sequence below the iron formation. This low temperature hydrothermal event enriched the footwall sequence in Fe, K and Mn at ~1650 Ma, and its spatial association with metre-scale BIFs provides circumstantial evidence that this occurred during sedimentation. The F enrichment of the unit conjecturally developed later during the Cu-Au ore event, with preferential F uptake by pre-existing biotite. A more detailed structural model for ore formation is outlined below.

Structural Factors

The ore event is closely associated with D2.5, which regionally produced recumbent folds and a shallow-dipping foliation, indicating that the main stress field had a near-vertical σ_1 , a factor that must be considered for ore genesis models at this time. Evidence presented indicates that D2.5 generated moderately strong crenulations through the ore sequence, as well as broad dip changes of beds, and particularly, numerous zones of oblique and chocolate-block boudinage in and around the ore zone. These features are not present everywhere in the Eastern Succession (Bell, 1991; Pollard et al., 1997), so it is argued that Monakoff lies close to the hinge of a large D2.5 fold with a near-

horizontal axial trace. Development of S2.5 is associated with the formation of open parasitic folds. Monakoff Western Zone ore formed during the flexural slip, extension, and production of dilatancy in a broad D2.5 fold, a structural mechanism which accounts for the sheet-like ore geometry (parallel to bedding), and which has its best structural analogue in the saddle reefs and bedding parallel veins of slate-belt-hosted gold deposits, forming prior to fold lock-up (Cox et al., 1991). Fold lock-up also has the effect of causing strain accumulation due to the inability of the deforming sequence to accommodate the deformation and any changes in volume (eg., Davis et al., 2001b). Saddle reef mechanisms, and processes associated with the lock-up of both folds and thrusts, have been proposed for other Proterozoic gold-only deposits, such as parts of the Cosmopolitan Howley (Northern Territory, Australia), Telfer (Western Australia) and Sabie-Pilgrim's Rest (South Africa) deposits (Partington and McNaughton, 1997; Rowins et al., 1997; Harely and Charlesworth, 1992), and Archaean gold-only deposits such as Mulgarrie (Davis et al., 2001b). In these instances the axial planes are sub-vertical rather than sub-horizontal.

At Monakoff, strain was not distributed evenly across the package, but was focussed at unit contacts and older shear zones, with dilatancy occurring in those areas with near-vertical orientations. This is supported by the occurrence of mineralisation not only in the Monakoff Shear, but on numerous amphibolite-sediment contacts well into the footwall in DDH MKD2. However, a degree of pervasive fluid flow was also required, to account for the high geochemical background of fluorine and other ore elements in both the footwall and hangingwall.

The features of the boudin necks provide several constraints on the ore system. Firstly, the formation of boudin necks was synchronous with the arrival of ore fluid at the site,

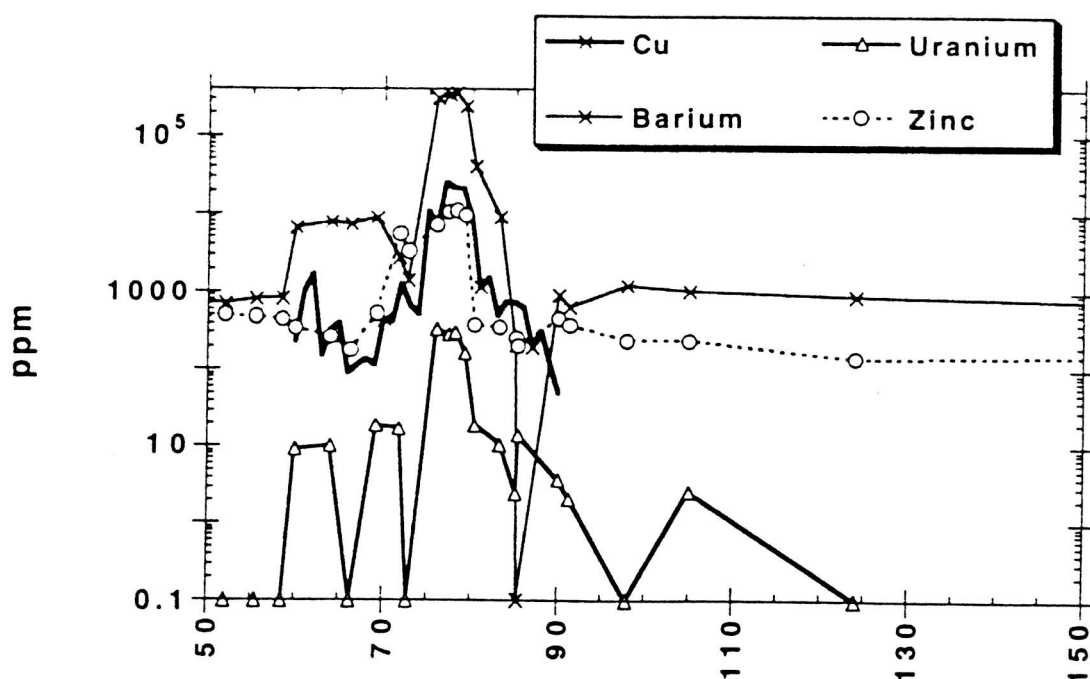


Figure 11: Downhole behaviour of Cu, Ba, Zn and U in MKD1.

because boudin necks contain many of the ore assemblages. Although this may be coincidence, it is more likely to be directly related to an increase in fluid pressures, increasing the probability of rupture on the failure envelope, resulting in movement of ore fluids into low mean stress sites offered by boudin necks. This is supported by the general lack of boudinage in the surrounding sequence, and by the curvilinear nature of associated fracture arrays within the metasomatic halo, which is symptomatic of brittle failure under high fluid pressures (McClay, 1987). Secondly, the enrichment of metals in many boudin-neck zones, each interpreted to have formed in a single failure episode, provides evidence that the ore forming fluid or fluids were extremely metal-rich, and consequently that ore deposition likely occurred in only a few failure episodes. Unfortunately the corrosive and reactive quality of the mineralising fluids obliterated much of the evidence of how the fluid infiltrated into the sequence to form the massive replacement orebodies.

Mineralogical and Geochemical Constraints

The fluid oxidation state during ore formation was high, to account for the dominance of sulphate in ores (S ~25–30%). Hematite is generally not observed except in the upper near-surface of the Monakoff Eastern Zone, where it forms large primary bladed crystals replacing amphibolite. Magnetite is the dominant iron oxide in the Western Zone, although there is doubt that it was precipitated at the same time as the ore, because of post-ore metamorphic recrystallisation. Magnetite grains at the margins of the ore zone were replaced by sulphide minerals. Oxidation-sensitive minerals mainly comprise pyrite, with minor pyrrhotite and arsenopyrite disseminated asystematically.

There is evidence in the whole rock geochemistry for more than one fluid at the time of ore formation. This arises from the abundant barite, fluorite and high background Mn; Ba does not have a high solubility in the presence of abundant dissolved sulphate, and the transport of both Mn and Ba is enhanced under reduced conditions (Cook et al., 2000). On the other hand, U transport is enhanced under oxidised conditions (Wilde et al., 1988) although the effect of F-complexing on U transport is not clear. The abundant barite could be accounted for: 1). from the mixing of a sulphate-rich oxidised fluid with a reduced Ba-bearing fluid; or 2). from the oxidation of a very reduced fluid to a sulphate-stable condition, thus precipitating barite. Option (2) is discounted because it should have produced large massive sulphide bodies, that are not evident. Option (1) could very effectively account for fluorite deposition by mixing of Ca-rich with F-rich fluids (Williams-Jones et al., 2000), although Bethke (1996) demonstrates that cooling is also an efficient depositional mechanism.

The small number of primary fluid inclusions that are available from mineralised open-growth sites do not contain daughter salts (consequently the fluids are <26.5 wt.% NaCl), but do possess variable L-V ratios, supporting mixing, boiling or syn-ore condensation. Given the brittle-ductile conditions of ore formation, boiling can be

discounted as a viable ore formation mechanism. Secondary inclusions do contain saline fluid inclusions with two daughter phases, but their timing with respect to mineralisation is not known.

The thermal conditions of ore formation are constrained by the stabilities of the alteration envelope phases of coexisting biotite and the almandine component of garnet. A broad estimate of 460–950° C is calculated for this assemblage in pelitic rocks (Ferry and Spear, 1978; Gessman et al., 1997). However, Mahar et al. (1997), Gessman et al. (1997) and others have found that high Mn stabilises garnet below its normal range at higher and lower pressures in pelites, and additionally permits the growth of garnet at ~100° C below normal conditions, so that these thermal constraints will be adjusted with future precise work on garnet and biotite mineral chemistry (preliminary results are reported in Davidson and Davis, 1997 and 2001). The brittle-ductile behaviour during ore formation favours pressures of ~3 kBar, which is consistent with regional estimates of pressures (Jaques et al., 1982) for the northern Eastern Succession between D2 and D3, a likely period of episodic uplift (O'Dea et al., 1997).

An Integrated Genetic Model

The early syn-sedimentary hydrothermal history influenced the bulk geochemical character of the sequence that was leached during the subsequent metamorphic history. This low temperature hydrothermal event enriched the footwall sequence in Fe, K and Mn at ~1650–1640 Ma, and produced metre-scale BIFs over a large area; it may have had a broad relationship with Broken Hill-type deposit formation, which some workers interpret to have accompanied Soldiers Cap Group sedimentation (Bodon, 1998; Walters and Bailey, 1998). All lithologies in the ore sequence were emplaced during sedimentation, with the exception of a narrow sub-alkaline dolerite dyke.

The structural history involved the development of a narrow shear system by strain partitioning around rigid blocks of mafic igneous rocks during D1, with folding and mild reactivation in a regionally unusual orientation during D2, producing the broad east-west oriented Pumpkin Gully Syncline (Fig. 12). Steeply plunging F2 folds are a product of both the steep dips imposed upon the sequence during D1, and the variation in D2 strain along the hinge line of the folds. These local events were part of a regional duplexing of the Mary Kathleen Group meta-carbonates and evaporites, with the dominantly clastic carbonate-poor Soldiers Cap Group rocks; a tectonic contact between these packages is hypothesised to deeply underlie the Pumpkin Gully Syncline (O'Dea et al., 1997 and references therein). Mild vertical compression reactivated the Monakoff Shear system during D2.5, ie. at ore-time.

Flexural slip during D2.5 was concentrated on the east-west, near vertical, D1 shear system, with fluid packages being drawn in by extensional failure resulting in transient low pressure sites. High fluid pressures enhanced the local development of extensional failure by boudinage. During

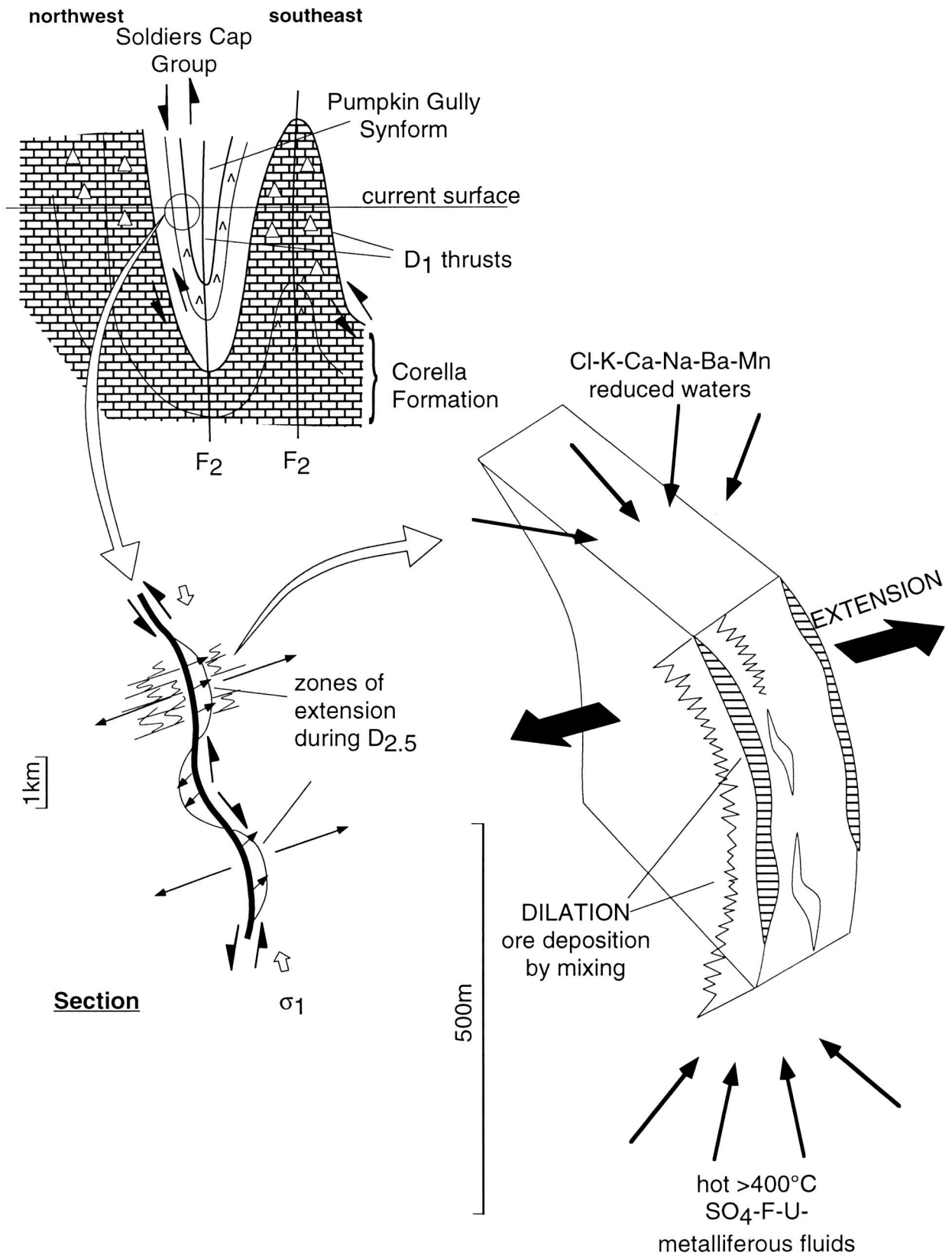


Figure 12: Genetic model for Monakoff, involving dilation in a broad D_{2.5} hinge zone, which induced mixing of a metal-bearing, >400° C, F-S-metal-rich fluid (granite derived?), with a reduced Ca-K-Ba rich fluid (meta-evaporite-derived), stimulating sulphide, barite and fluorite deposition.

D2.5, steeply plunging F2 folds (and hinge breccias) adjacent to dilating shear surfaces also channelled some fluids into the D2 hinge zones, producing pipe-like mineralisation zones. These pipes likely pinch and swell at depth, due to different dilational behaviour of changing D2 fold-plunge during D2.5. The geometry of extension during D2.5 favoured the inflow and mixing of fluids from above and below, producing a pronounced thermal anomaly compared to the temperatures of surrounding metamorphic rocks. The paragenesis indicates that an early stage (Stage 1) of high temperature alkali metasomatism formed knots of massive magnetite surrounded by a shell of biotite 1 within the D1 shear system. Conditions of formation for stage 1 are not well constrained, but the assemblage characterises the early hydrothermal history of many shears in the vicinity of the Naraku Batholith, most notably at Ernest Henry, where they provide much of the magnetic response that initially attracted the attention of explorers (Craske, 1995). The breakdown of Stage 1 magnetite to form sulphide minerals is evidence that Stage 1 products may have played a role in ore precipitation. Stage 1 magnetite replaces D1 foliations and D2 folds, but its relationship to D2.5 could not be ascertained. In the Eastern Succession, control of later hydrothermal deposition by reaction with earlier hydrothermal products was first noted at the Eloise Cu-Au deposit by Baker (1994, 1998).

Stage 2 of the hydrothermal system was responsible for most ore and alteration assemblages. Mixing in dilatant zones was critical to the formation of abundant ore-stage barite, since Ba and oxidised S transport is not effective within the same fluid (Cooke et al., 2000). The proposed fluid chemistry was:

Fluid 1 - reduced, Ca-K-Fe-Mn-Ba rich, CO₂-rich, and saline, buffered mainly to the Mary Kathleen Group carbonates at regional metamorphic temperatures.

Fluid 2 - sulphate-rich, metal-bearing, 400–600° C, and F-rich. To account for the high F, fluid 2 may have been granite derived.

Mixing of these fluids deposited abundant barite, and possibly anhydrite (subsequently replaced by carbonate). The reaction of fluid 2 with earlier disseminated magnetite and Fe²⁺-rich assemblages, acted to increase the concentration of H₂S available for sulphide deposition. However, an important feature of the mixing was the destabilisation of metal- and REE-F complexes when abundant fluorite deposition was stimulated by mixing with the calcic fluids. Such destabilisation may also have occurred where the wallrocks themselves were very calcic, which may account for the preferential replacement of amphibolite in the Monakoff Eastern Zone.

Very high metal concentrations in fluid 1 are suggested by: 1). the occurrence of high metal abundances in one-pass fluid circulation systems such as boudin neck zones; and 2). metal deposition at extreme temperatures, where most metals are still under-saturated. To account for the presence of hematite in some areas, and pyrrhotite in others, steep oxidation gradients must have been present on local scales,

with hematite-stable zones representing the most oxidised parts of the system. CO₂-gradients, likely also displaced carbonate for hematite, because the stability field of Fe-Mn carbonate is enhanced by high pCO₂ relative to hematite under oxidised conditions at low to moderate temperatures (Cooke et al., 2000). This may also account for the general lack of hematite in an otherwise very oxidised environment at Monakoff.

Paragenetic Contrasts to the Ernest Henry Cu-Au Deposit

Ernest Henry exhibits the following alteration events, summarised from Mark et al. (2000) (and given new titles for ease of reference here), in order of occurrence:

Stage 1 - Regional Na-Ca alteration;

Stage 2 - Pre-ore disseminated biotite-magnetite alteration up to kilometres from the deposit, and spessartine-K feldspar (Ba)-manganiferous biotite veining transitional to the ore event;

Stage 3 - K-feldspar-hematite alteration transected by quartz-calcite-magnetite-fluorite-titanite/rutile veins) within 2 km of ore, transitional to two ore vein and breccia matrix stages consisting of magnetite, calcite, pyrite, biotite, chalcopyrite, K feldspar, titanite and quartz, with accessory garnet, barite, molybdenite, fluorite, amphibole, apatite, monazite, arsenopyrite, LREE fluoro-carbonate, galena, cobaltite, sphalerite, scheelite, uraninite and tourmaline;

Stage 4 - Post-ore carbonate 'flooding', forming veins and breccias of carbonate-quartz-biotite-actinolite-pyrite-magnetite-minor garnet-chalcopyrite.

In comparison, Monakoff is missing the early regional Na-Ca alteration, but conspicuous albite alteration post-dates all other types (Monakoff Stage 4), and is focussed on NW-trending faults. Most obviously, the massive K-feldspar-hematite alteration which is the hallmark of Ernest Henry ore and alteration is absent from Monakoff. However, the abundant biotite in Monakoff Stages 1 and 2 attests to similar K-metasomatism during and prior to the ore events. Conditions of alteration are likely to have been more reduced at Monakoff compared to Ernest Henry, thus stabilising biotite-magnetite over K-feldspar-hematite. Additionally, fluid flow at Monakoff was highly partitioned and subjected to lower fluid pressures, on the basis of the confinement of ore formation and alteration to the major zones of structural weakness, and the far lower abundance of fluid-related brecciation.

Exploration implications

Our improved structural understanding of the Monakoff deposit provides potential new target areas in the district. Ore forms a 1.5 km long sheet which is basically continuous to the north-south fault (to the west), and to the east extends to a large D2 fold, which is now offset in a left-lateral sense by a D3 fault (Fig.1 and Fig. 3). This compartment may have experienced dilation across its whole length during D2.5, with the greatest dilation occurring near the centre of the sheet. The western fault may either have accommodated

shearing strain if it was present during D2.5, or more likely it offset the mineralisation obliquely as well as in a strike-slip sense, such that mineralisation does not now continue to the west. To the east, D2.5 dilation may have been interrupted by the medium-scale D2 fold zone, but repetitions could be expected at the intersection between D2.5 fold hinges and steeply-dipping D1 shear positions to the east, and within amphibolite in reactivated D2 fold hinges.

Previous exploration attention has mainly focussed on the magnetic and outcropping BIFs, but this study indicates the importance of early steep shears, steep lithological contacts, and large-scale inhomogeneities in competency, as alternate targets. Notably the structural-aeromagnetic interpretation suggests the occurrence of fault repetitions of the ore package several kilometres to the north east under cover (Fig. 1). Broadly the model would favour ore positions close to Mary Kathleen Group/Soldiers Cap Group contacts, to facilitate fluid mixing. Given the probable granitic fluid source for F, sub-surface granites close to D2.5 dilational sites should be targeted, but other than a post-D2.5 thermal peak (evidenced by randomly oriented disseminated biotite 3 throughout the area), there is no surface evidence of granites within 2 km of Monakoff. The obvious conduit to these granites is a north-south vertical fault system 1 km west of Monakoff, but the timing of this fault is not known, other than it contains probable D3-age carbonate-vein systems.

Comparison with the Ernest Henry paragenesis indicates that widespread or intense K feldspar alteration is not a prerequisite to form the polymetallic element assemblage that characterises both Ernest Henry and Monakoff. We do not yet know whether the more oxidised style of K-metasomatism at Ernest Henry, and the higher fluid pressures that resulted in extensive brecciation, were critical features in the formation of large tonnages there, compared to Monakoff.

Acknowledgements

This work was supported by collaborative ARC-AMIRA Project P438, an Australian Post-doctoral Research Fellowship for BKD, and an Australian Research fellowship for GJD. Cloncurry Mining, and in particular Steve Milner, Jim and Annette, and Julie Hugenholtz, kindly allowed access and provided logistical support. Simon Stephens, Wieslaw Jablonski, Debbie Harding and Sharon Ness (JCU) all assisted in production of the many numbers and figures in this paper. Discussions with Peter Pollard, Pat Williams, Kevin Blake, James Lally and many JCU post-graduate students improved our understanding of the Monakoff system, in its context as a small part of Mt Isa Inlier hydrothermal activity. Lastly, a firm thankyou! to all of the companies and their geologists who financially supported this project, and encouraged us during our fieldwork and reporting.

References

- Adshead, N.D., 1995 - Geology, alteration and geochemistry of the Osborne Cu-Au deposit, Cloncurry district, NW Queensland, Australia. Unpublished Ph.D thesis (James Cook University), 382 p.
- Ashley, P.M., 1983 - Recent exploration results at the Monakoff prospect, near Cloncurry, northwest Queensland. Esso Minerals internal report, Dec. 1983 (held by Terra Search, Townsville).
- Baker, T., 1994 - Localization of sulphides by a hornblende-biotite alteration system at the Eloise Cu-Au deposit, Cloncurry district, NW Queensland. Geological Society of America 1994 abstracts with programs, A-379.
- Baker, T., 1998 - Alteration, mineralization and fluid evolution at the Eloise Cu-Au deposit, Cloncurry district, northwest Queensland, Australia. *Economic Geology* 93, 1213–1236.
- Beardsmore, T.J., Newbery, S.P. and Laing, W.P., 1988 - The Maronan Supergroup— an inferred early volcanosedimentary rift sequence in the Mount Isa Inlier, and its implications for ensialic rifting in the Middle Proterozoic of northwest Queensland. *Precambrian Research* 40/41, 487–507.
- Bell, T.H., 1991 - The role of thrusting in the structural development of the Mt Isa Mine and its relevance to exploration in the surrounding region. *Economic Geology* 86, 1602–1625.
- Bethke, C.M., 1996 - Geochemical reaction modelling. Oxford University Press, New York, 397 p.
- Bodon, S. B., 1998 - Paragenetic relationships and their implications for ore genesis at the Cannington Ag-Pb-Zn deposit, Mt Isa Inlier, Queensland, Australia. *Economic Geology* 93, 1463–1488.
- Cooke, D.R., Bull, S.W., Large, R.R. and McGoldrick, P.J., 2000 - The importance of oxidized brines for the formation of Australian Proterozoic stratiform sediment-hosted Pb-Zn (Sedex) deposits. *Economic Geology*, 95, 1–18.
- Cox, S.F., Wall, V.J., Etheridge, M.A. and Potter, T.F., 1991 - Deformational and metamorphic processes in the formation of mesothermal vein-hosted gold deposits— examples from the Lachlan Fold Belt in central Victoria, Australia. *Ore Geology Reviews* 6, 391–423.
- Craske, T., 1995 - Geological aspects of the discovery of the Ernest Henry Cu-Au deposit, northwest Queensland. *Australian Institute of Geologists Bulletin* 16, 95–109.

- Davidson G.J., 1994 - A geochemical and geological reconnaissance study of alteration, copper-gold ores, and iron-rich lithologies in the Cloncurry area, Mt Isa Inlier. Unpublished CODES report, March 1994, University of Tasmania, 185p.
- Davidson, G.J., 1995 - Progress Report 1: Monakoff—macroscopic geology in Pollard, P. (compiler) Cloncurry base metals and gold annual report, October 1995, AMIRA P438, 3A-1/3A-10.
- Davidson G.J., 1998 - Variation in copper-gold styles through time in the Proterozoic Cloncurry goldfield, Mt Isa Inlier: a reconnaissance view. *Australian Journal of Earth Sciences*, 45, 445-462.
- Davidson, G.J. and Davis, B.K., 1996 - Progress report 2: Monakoff— S isotope geochemistry and descriptive structural geology. Cloncurry base metals and gold annual report, October 1996, AMIRA P438, 8-1-8-13.
- Davidson, G.J. and Davis, B.K., 1997 - Characteristics of the Monakoff Cu-Au-F-Ba-Mn deposit, Mt Isa Eastern Succession. Final report Cloncurry base metals and gold project, September 1997, AMIRA P438, 13-1-13-53.
- Davidson, G.J. and Davis, B.K., 2001 - Structural and geochemical constraints on the emplacement of the oxide Cu-Au Monakoff deposit. In: Williams, P.J., ed., *A Hydrothermal Odyssey*, Townsville, 17-19th May 2001, EGRU Contribution 59, 44-45.
- Davidson, G.J. and Large, R.R., 1998 - Proterozoic Au-Cu deposits. *AGSO Journal Jubilee Papers*, 17, 105-114.
- Davis, B.K., Pollard, P.J., Lally, J.H., McNaughton, N.J., Blake, K. and Williams, P.J., 2001a - Deformation history of the Naraku Batholith, Mt Isa Inlier, Australia: implications for pluton ages and geometries from structural study of the Dipvale Granodiorite and Levian granite. *Australian Journal of Earth Sciences* 48, 113-129.
- Davis, B.K., Hickey, K.A. and Rose, S., 2001b - Superposition of gold mineralisation on pre-existing carbonate alteration: structural evidence from the Mulgarrie gold deposit, Yilgarn Craton. *Australian Journal of Earth Sciences* 48, 131-149.
- Deer, W.A., Howie, R.A. and Zussman, J., 1992 - *An introduction to the rock-forming minerals*. Longman, Hong Kong.
- De Jong, G., and Williams, P.J., 1995 - Evolution of metasomatic features during exhumation of mid-crustal Proterozoic rocks in the vicinity of the Cloncurry Fault, NW Queensland. *Australian Journal of Earth Sciences* 42, 281-290.
- Derrick, G.M., 1996 - The 'geophysical approach to metallogeny of the Mt Isa Inlier. Proceedings of the Australasian Institute of Mining & Metallurgy Annual Conference, Perth, 24-28 March, 1996, 349-366.
- Derrick, G.M., Wilson, I.H. and Hill, R.M., 1976 - Revision of stratigraphic nomenclature in the Precambrian of northwestern Queensland. V. Soldiers Cap Group. *Queensland Government Mining Journal* 77: 600-604.
- Dong, G., 1996 - Fluid inclusions from Cloncurry ore systems. Cloncurry base metals and gold annual report, September 1996, AMIRA P438, 5-1/5-17.
- Ferry, J.M. and Spear, F.S., 1978 - Experimental calibration of the partitioning of Fe and Mg between biotite and garnet. *Contributions to Mineralogy and Petrology*, 66, 113-117.
- Garrett, S., 1992 - Geology and geochemistry of the Mount Elliott copper-gold deposit, N.W. Queensland. Unpublished M.Sc thesis, University of Tasmania, 139 p.
- Gessman, C.K., Spiering, B. and Raith, M., 1997 - Experimental study of the Fe-Mg exchange between garnet and biotite: constraints on the mixing behaviour and analysis of the cation-exchange mechanisms. *American Mineralogist* 82, 1225-1240.
- Harely, M. and Charlesworth, E.G., 1992 - Thrust-controlled gold mineralization at the Elandshoogte mine, Sabie-Pilgrim's Rest goldfield, South Africa. *Mineralium Deposita* 27, 122-128.
- Hatton, O.J., Bull, S.W. and Davidson, G.J., 2000 - A review of the geological setting and sedimentology of the Proterozoic upper Soldiers Cap Group, Eastern Succession, rift fill in a Pb-Zn-rich basin (Mt Isa Inlier, NW Queensland). Proceedings of New Ideas for a New Millennium, Cranbrook Workshop, May 6-7 2000. <http://www.cyberlink.bc.ca/~ekcm/Abstracts.htm>
- Jaques, A., Blake, D. and Donchak, P., 1987 - Regional metamorphism in the Selwyn Range area, northwest Queensland. *Australian Bureau of Mineral Resources Journal of Geology & Geophysics* 7, 181-196.
- Laing, W., 1991 - Base metal + gold mineralisation styles in the Cloncurry terrane. *Economic Geology Research Unit Contribution* 38: 77-88.
- Macready, T., Goleby B.R., Goncharov, A., Drummond, B.J. & Lister, G.S., 1998 - A framework of overprinting orogens based on the interpretation of the Mount Isa deep seismic transect. *Economic Geology* 93, 1422-1434.
- Mahar, E.M., Baker, J.M., Powell, R., Holland, T.J.B. and Howell, N., 1997 - The effect of Mn on mineral stability in metapelites. *Journal of Metamorphic Geology* 15, 223-238.

- Mark, G., 1998 - Albitite formation by selective pervasive sodic-alteration of tonalite plutons in the Cloncurry district, NW Queensland. *Australian Journal of Earth Sciences* 45, 765–774.
- Mark, G., Oliver, N.H.S., Williams, P.J., Valenta, R.K., Crookes, R.A., 2000 - The evolution of the Ernest Henry Fe-oxide-(Cu-Au) hydrothermal system; In Porter T.M., Ed., *Hydrothermal iron oxide copper-gold & related deposits*, Australian Mineral Foundation, Adelaide, 123–136.
- Marshall, L.J. and Oliver, N.H.S., 2001 - Regionally extensive tectonic and hydrothermal breccias in the Cloncurry Fe-oxide-Cu-Au district, NW Queensland. In: Williams, P.J., ed., *A Hydrothermal Odyssey*, Townsville, 17–19th May 2001, EGRU Contribution 59, 126–127.
- McClay, K., 1987 - The mapping of geological structures. *Geological Society of London handbook series*, Wiley & Sons, Chichester, 161 p.
- Milner, S., 1993 - The Monakoff Cu-Pb-Zn-Au-Ag-Co-Ba-F deposit—geological summary. In: Derrick, G., ed., *Core Shack Explanatory Notes*, AMF Course 832/93, Australian Mineral Foundation, Glenside, South Australia, 31–39.
- Munöz, J.L., 1984 - F-OH and Cl-OH exchange in mica with applications to hydrothermal ore deposits. In: Bailey, S.W., ed., *Micas. Reviews in Mineralogy* 13, 469–491.
- O’Dea, M.G., Lister, G.S., MacCready, T., Betts, P.G., Oliver, N.H.S., Pound, K.S., Huang, W. and Valenta, R.K., 1997 - Geodynamic evolution of the Proterozoic Mount Isa terrain; In: Burg, J.-P. and Ford, M., eds., *Orogeny through time*, Geological Society Special Publication 121, 99–122.
- Oliver, N.H.S., 1995 - Hydrothermal history of the Mary Kathleen Fold Belt, Mt Isa Block, Queensland. *Australian Journal of Earth Sciences* 42, 267–280.
- Page, R.W., 1988 - Geochronology of early to middle Proterozoic fold belts in northern Australia: a review. *Precambrian Research* 40/41, 1–19.
- Page, R.W. and Sun, S-s, 1998 - Aspects of geochronology and crustal evolution in the Eastern in the Eastern Fold Belt, Mount Isa Inlier. *Australian Journal of Earth Sciences* 45, 343–362.
- Partington, G.A. and McNaughton, N.J., 1997 - Controls on mineralization in the Howley district, Northern Territory: a link between granite intrusion and gold mineralization. *Chron. Rech. Min.*, 529, 25–44.
- Pollard, P.J., Davis, B.K. and Williams, P.J., 1997 - Structural and physicochemical controls on ore formation in Cloncurry Cu-Au deposits, eastern Mount Isa Inlier, Queensland. Final report Cloncurry base metals and gold project, September 1997, AMIRA P438, 2-1–2-41.
- Pollard, P.J., Mark, G. and Mitchell, L.C., 1998 - Geochemistry of post-1540 Ma granites in the Cloncurry district, northwest Queensland. *Economic Geology* 93, 1330–1344.
- Reeve, J.S., Cross, K.C., Smith, R.N. and Oreskes, N., 1990 - Olympic Dam copper-uranium-gold-silver deposit; In: Hughes F.E., ed., *Geology of the mineral deposits of Australia and Papua New Guinea: Australasian Institute of Mining & Metallurgy Mon. 14*, p. 1009–1035, Melbourne, Australia.
- Reinhardt, J., 1987 - Cordierite-anthophyllite rocks from north-west Queensland, Australia: metamorphosed magnesian pelites. *Journal of Metamorphic Geology* 5: 451–472.
- Ronzê, P.C., Soares, A.D.V., dos Santos, G. S. and Barreira, C.F., 2000 - Alemão copper-gold (U-REE) deposit, Carajás, Brazil; In Porter T.M., Ed., *Hydrothermal iron oxide copper-gold & related deposits*, Australian Mineral Foundation, Adelaide, 191–202.
- Rotherham, J. F., 1997 - A metasomatic origin for the iron-oxide Au-Cu Starra orebodies, Eastern Fold Belt, Mt Isa Inlier. *Mineralium Deposita* 32, 205–218.
- Rowins, S.M., Groves, D.I., McNaughton, N.J., Palmer, M.R. and Steward, C.S., 1997 - A reinterpretation of the role of granitoids in the genesis of Neoproterozoic gold mineralization in the Telfer Dome, Western Australia. *Economic Geology* 92, 133–160.
- Rubenach, M.J. and Barker, A.J. 1996 - Episodic metamorphism and metasomatism in pelitic rocks of the Snake Creek Anticline; In: Baker, T., Rotherham, J., Richmond, J., Mark, G. and Williams, P., eds., *MIC ’96 New developments in metallogenic research: the McArthur, Mt Isa, Cloncurry minerals province*; EGRU Contribution 55, 127–130.
- Ryburn, R.J., Wilson, I.H., Grimes, K.G. and Hill, R.M., 1988 - Cloncurry 1:100 000 geological map commentary. Australian Bureau of Mineral Resources.
- Souza, L.H. and Vieira, E.A.P., 2000 - Salobo 3 Alpha deposit: geology and mineralisation ; In Porter T.M., Ed., *Hydrothermal iron oxide copper-gold & related deposits*, Australian Mineral Foundation, Adelaide, 213–224.
- Tazava, E. and de Oliveira, C.G., 2000 - The Igarapé Bahia Au-Cu-(REE-U) deposit, Carajás Mineral Province, Northern Brazil ; In Porter T.M., Ed., *Hydrothermal iron oxide copper-gold & related*

deposits, Australian Mineral Foundation, Adelaide, 203–212.

Walters, S. and Bailey, A., 1998 - Geology and mineralization of the Cannington Ag-Pb-Zn deposit: an example of Broken Hill-type mineralization in the eastern Succession, Mount Isa Inlier, Australia. *Economic Geology* 93, 1307–1329.

Wilde, A.R., Bloom, M.S., Wall, V.J., 1989 - Transport and deposition of gold, uranium and platinum-group elements in unconformity-related uranium deposits. *Economic Geology Monograph* 6, 637–650.

Williams, P.J., 1998 - An introduction to the metallogeny of the McArthur River-Mount Isa-Cloncurry minerals province. *Economic Geology* 93, 1120–1131.

Williams-Jones, A.E., Samson, I.M. and Olivo, G.R., 2000 - The genesis of hydrothermal fluorite-REE deposits in the Gallinas Mountains, New Mexico. *Economic Geology* 95, 327–342.

Winchester, J.A. and Floyd, P. A., 1977 - Geochemical discrimination of different magma series and their differentiation products using immobile elements. *Chemical Geology* 20, 325-343.

Wyborn, L.A.I., 1998 - The younger ca 1500 Ma granites of the Williams and Narku Batholiths, Cloncurry district, eastern Mt Isa Inlier: geochemistry, origin, metallogenic significance and exploration indicators. *Australian Journal of Earth Sciences* 45, 397–412.

